# Two-Surfaces Sliding Mode Controller for Energy Management of Electric Vehicle Based on Multi Input DC-DC Converter

**P. Bayat[1], H. Mojallali[2,*], A. Baghramian[3], P. Bayat[4]**

Electrical Engineering Department, Faculty of Engineering, University of Guilan, Rasht, Iran

mojallali@guilan.ac.ir

**Abstract**

In this paper, a two-surfaces sliding mode controller (TSSMC) is proposed for the voltage tracking control of a two input DC-DC converter in application of electric vehicles (EVs). The imperialist competitive algorithm (ICA) is used for tuning TSSMC parameters. The proposed controller significantly improves the transient response and disturbance rejection of the two input converters while preserving the closed-loop stability. The combination of the proposed controller and ICA, realizes a fast transient response over a wide transient load changes and input voltage disturbances. For modeling the equations governing the system, state-space average modeling technique is used. In order to analyzing the results, the two input converter equipped with the proposed controller, was modeled in MATLAB/SIMULINK environment. Simulation results are reported to validate the theoretical predictions and to confirm the superior performance of the proposed nonlinear controller when it is compared with a conventional pure SMC.

***Keywords****: Electric vehicles (EVs), Imperialist competitive algorithm (ICA), Two-surfaces sliding mode controller (TSSMC), Two input DC-DC converter.*

## 1. Introduction

In recent decades, electric vehicles (EVs) have improved their performance and are suitable for commercial use instead of conventional fuel vehicles. However, due to the limited battery capacities, EVs still suffer from the main problem of shorter driving range compared with fuel vehicles [1]. In all sources of EVs, their available energy varies in a random manner resulting a wide variation in the available output voltage and power, furthermore the voltage provided by the sources decrease during their discharging. To provide a constant voltage to the electronic system during the whole sources runtime, the sources voltage must be regulated by a DC–DC converter; due to these situations, the power converter is a necessary part of the EVs.

To integrate hybrid DC energy sources of different types to a power storage such as battery and supercapacitors (SCs), multi input DC-DC converters are commonly used to step up low level source voltages to a constant high level voltage that is required by a system. Comparing to that solution, a two input bidirectional DC-DC converter is preferable owing to the advantages of using fewer components, lower cost, higher power density, and higher efficiency [1,2]. The two input converter topologies can be classified into non-isolated and isolated topologies [3]. Non-isolated two input converters are usually used in the applications where a low voltage regulation ratio is required [4,5]. In contrast, in the applications requiring a high voltage regulation ratio, isolated converters which contains a transformer is preferred [6,7].

Recently, two input topology were proposed by adding one middle branch to the conventional half-bridge converter [8,9], furthermore by combining any two of the three basic converters (buck, boost, and buck-boost converter), a family of novel two-inductor two input DC–DC converters are proposed in [10,11]. These converters use only one switch to manage the power distribution among the three ports, which reduces the size and cost of the converter significantly. It uses less controllable power switches than the half-bridge topology and can achieve soft switching for all main switches. However, the voltage of the primary source should be maintained at a high

value to charge the battery and the battery is both charged and discharged within a switching period. Such a high-frequency charge/discharge has a negative effect on the battery lifetime.

A novel non-isolated two input converter is proposed in [12] by combining a traditional boost converter and a buck converter. Ref. [13] proposed a two input energy storage system (ESS) by using a traditional buck-boost converter which analyzed in detail in [14].

The controller is an important part of the most converters. Designing a good controller with an acceptable transient and steady-state performance is an effortful process because of the highly non-linear dynamics and non-minimum phase structure of the most converters [15–17]. Many kinds of controllers, namely linear, [18–20] non-linear [21–23], and intelligent [16, 24–26] methods have been offered for the control of the energy management systems (EMSs). Although the linear controllers, such as proportional integral (PI) and PI derivative (PID) could have been established with an acceptable performance around the selected operating point, their performance might be declined when the operating point of the system is changed [15, 27–29].

To increase the effectiveness of the PI or PID controller devoted for the converter, various kinds of the auto gain tuning methods were proposed in [30–32]. However, the controller design processes of these methods are more complicated than the classical PI/PID control methods. In several studies, it was demonstrated that the intelligent methods, such as neural network [24], fuzzy logic [25, 27], queen bee, and genetic algorithm [26] dedicated for the control of the converter have a suitable performance.

In addition to the acceptable transient and steady-state behavior, the controller devoted to control converter should also be robust to disturbances, such as variations in the load resistance and input voltage which may occur naturally during operation of the converter. Various control methods were offered to achieve a robust converter structure. The robustness of the controller against variation in the load and the line disturbances was explored by using linear matrix inequalities [33,34], H2 [35], H∞ and sliding mode controller (SMC) [36,37] approaches.

Ref. [38] designed and analyzed a simple novel control strategy for a hybrid ESS. Ref. [39] presented the utilization of an ESS device consisting of a SC bank for future EVs with a hydrogen fuel cell (FC) as the main power source and mainly focused on the innovative control law based on the flatness properties for a FC/SC hybrid power source. In [40], a control method of energy management based on SMC is proposed. This method, not only maintains the DC bus voltage of the hybrid ESS but also makes the SC voltage work in a proper limited range.

SMC is an alternative method of designing the control loop of parallel systems controlled by democratic or master-slave current-control schemes. Essentially, the SMC utilizes a high-speed switching control law to drive the nonlinear state trajectory onto a specified surface in the state space, called the sliding or switching surface, and to maintain it on this surface for all subsequent time [41]. The main feature of the sliding mode is the robustness that the system acquires against disturbances in the load and in the input voltage [42], [43].

In this paper as shown in Figs. 1 and 2, for controlling ESS and having smaller current ripple for the battery and SCs, a two-surfaces sliding mode controller (TSSMC) was proposed for two input bidirectional DC-DC converter. The proposed controller used two-surfaces, one for SC port and another for battery port. The imperialist competitive algorithm (ICA) is used for tuning TSSMC parameters. The proposed controller significantly improves the transient response and disturbance rejection of the two input converters while preserving the closed-loop stability and improving EVs efficiency.

The combination of the proposed controller and ICA operation over a wide load range, narrowed regulating frequency range, robustness, and fast transient response against transient load changes. For modeling the equations governing the system, state-space average modeling technique was used. Simulation results are reported to validate the theoretical predictions and to confirm the superior performance of the proposed nonlinear controller when it is compared with a conventional pure SMC.

The rest of this paper is organized as follows: dynamic modeling of two input converter extracted in Section II. A TSSMC will be designed, in Section III. In Section IV, the dynamic models are described for parts of proposed EMS. In Section V, the simulation results for the proposed EMS will be presented and compared. In Section VI, the conclusions of this paper will be stated.

## 2. Dynamic Modeling of Two Input Converter

There are many methods to achieve dynamic modeling of power converters and in this paper, the state space averaged model for the hybrid ESS was used. The model is derived based on the well-known averaging method initiated by Middlebrook in [44]. The two MOSFETs S1 and S2 operate synchronously, when one is off, the other is on. Similarly with S3 and S4. Let the switching period be Ts, the duty cycle for

the on state of S2 be D1 and the duty cycle for the on-state of S4 be D2.

The circuit has two state variables for SC port and three state variables for battery port, as marked in Figs. 3 and 4. The state variables, usually the inductors current and the capacitors voltage, are represented in the vector X.

State space average modeling method for SC port

In Fig. 3, the half-bridge SC cells is shown in two different modes. The equations governing the system has been extracted in (1)-(21), then sort out these formulas based on state space variables and the state space is extracted according to (4) and (10). Transfer function of the output voltage (Vout) to D has been extracted in (21). Parameter values shown in table I are used in transfer function (21) for dynamic investigation.

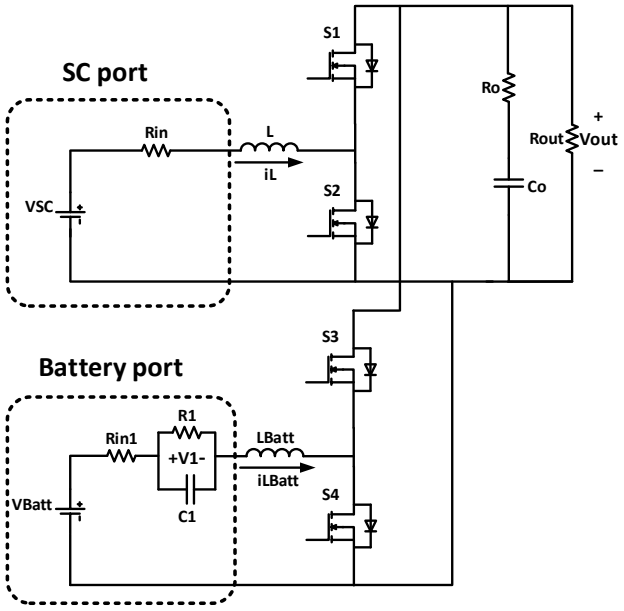


**Fig1.**. Energy exchange between SCs, battery pack and load considering two input bidirectional converter

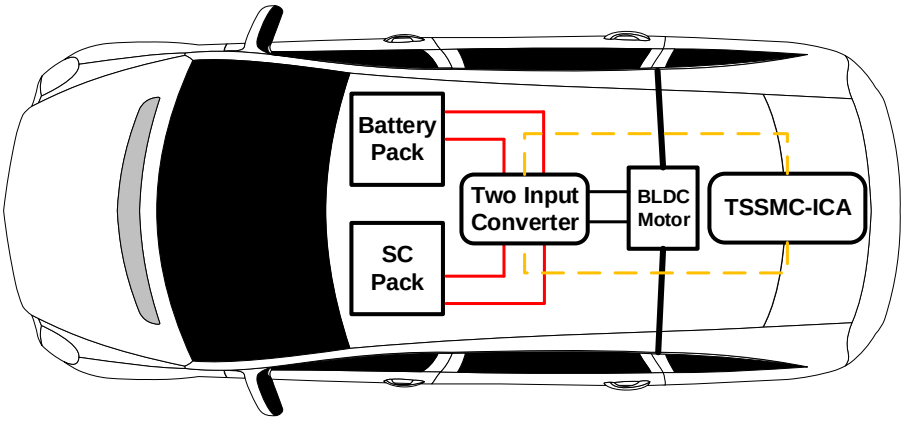


**Fig2.** Fig. 2. EMS with battery pack, SCs and two input bidirectional converter

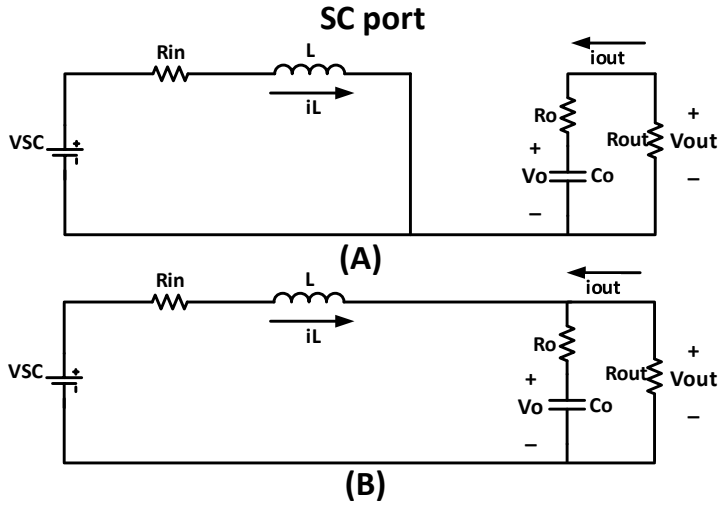


**Fig3.** Two operating modes of the SC port

**Table. I.** Parameters of the two converters

| Parameters | Value |
|---|---|
| Rin (for SC) | 0.04 Ω |
| L, $L_{Batt}$ | 32 μH |
| Rin (for Battery) | 0.11 Ω |
| R1 | 0.25 Ω |
| C1 | 0.22 μF |
| Co | 1 μF |

\\

$$X = \begin{bmatrix} V_o \\ i_L \end{bmatrix}, U_i = \begin{pmatrix} I_{out} \\ V_{SC} \end{pmatrix} \quad (1)$$

For Fig. 3.A the equations are:

$$V_{SC} = R_{in} i_L + L\frac{di_L}{dt} \Rightarrow \frac{di_L}{dt} = \frac{1}{L}V_{SC} - \frac{R_{in}}{L} i_L \quad (2)$$

$$V_{out} = R_o I_{out} + V_o \quad \& \quad \frac{dV_o}{dt} = \frac{1}{C_o} I_{out} \quad (3)$$

So:

$$V_{out} = R_o I_{out} + R_o I_L + V_o \quad (7)$$

$$\begin{bmatrix} \frac{dV_o}{dt} \\ \frac{di_L}{dt} \end{bmatrix} = A_1 \begin{bmatrix} V_o \\ i_L \end{bmatrix} + B_1 \begin{bmatrix} I_{out} \\ V_{SC} \end{bmatrix} = \quad (4)$$

$$\begin{bmatrix} 0 & 0 \\ 0 & -\frac{R_{in}}{L} \end{bmatrix} \begin{bmatrix} V_o \\ i_L \end{bmatrix} + \begin{bmatrix} \frac{1}{C_o} & 0 \\ 0 & \frac{1}{L} \end{bmatrix} \begin{bmatrix} I_{out} \\ V_{SC} \end{bmatrix}$$

For Fig. 3.B the equations are:

$$I_{out} + i_L = C_o \frac{dV_o}{dt} \Rightarrow \frac{dV_o}{dt} = \frac{1}{C_o} I_{out} + \frac{1}{C_o} i_L \quad (5)$$

$$V_{sc} = R_{in} i_L + L\frac{di_L}{dt} + V_{out} \quad (6)$$

From (6) and (7), obtained:

$$V_{sc} = (R_{in} + R_o) i_L + L \frac{di_L}{dt} + V_o + R_o I_{out} \quad (8)$$

$$\frac{di_L}{dt} = \frac{1}{L} V_{SC} - \frac{(R_{in} + R_o)}{L} i_L - \frac{V_o}{L} - \frac{R_o}{L} I_{out} \quad (9)$$

According to the (5) and (9):

$$\begin{bmatrix} \frac{dV_o}{dt} \\ \frac{di_L}{dt} \end{bmatrix} = A_2 \begin{bmatrix} V_o \\ i_L \end{bmatrix} + B_2 \begin{bmatrix} I_{out} \\ V_{PV} \end{bmatrix} = \quad (10)$$

$$\begin{bmatrix} 0 & \frac{1}{C_o} \\ -\frac{1}{L} & -\frac{(R_{in} + R_o)}{L} \end{bmatrix} \begin{bmatrix} V_o \\ i_L \end{bmatrix} + \begin{bmatrix} \frac{1}{C_o} & 0 \\ -\frac{R_o}{L} & \frac{1}{L} \end{bmatrix} \begin{bmatrix} I_{out} \\ V_{PV} \end{bmatrix}$$

$$\frac{V_{out}}{D(s)} = C\left[SI - A\right]^{-1}.[(A_1 - A_2).x + (B_1 - B_2)U_i] + (C_1 - C_2).x \quad (11)$$

$$A = A_1 D + A_2 (1 - D) \quad (12)$$

Then:

$$A = \begin{bmatrix} 0 & 0 \\ 0 & -D\frac{R_{in}}{L} \end{bmatrix} + \begin{bmatrix} 0 & \frac{1-D}{C_o} \\ \frac{D-1}{L} & \frac{(D-1)(R_{in} + R_o)}{L} \end{bmatrix} = \begin{bmatrix} 0 & \frac{1-D}{C_o} \\ \frac{D-1}{L} & \frac{DR_o}{L} - \frac{(R_{in} + R_o)}{L} \end{bmatrix} \quad (13)$$

where, in case of ideal converter $B_1 = B_2$ *and* $C_1 = C_2$ [44], so:

$$C_1 = C_2 = \begin{bmatrix} 0 & 1 \end{bmatrix}, C = \begin{bmatrix} 0 & D \end{bmatrix} + \begin{bmatrix} 0 & 1-D \end{bmatrix} = \begin{bmatrix} 0 & 1 \end{bmatrix} \quad (14)$$

From (11):

$$\frac{V_{out}}{D(s)} = \begin{bmatrix} 0 & 1 \end{bmatrix} \times \left[ \begin{bmatrix} s & 0 \\ 0 & s \end{bmatrix} - \begin{bmatrix} 0 & \frac{1-D}{C_o} \\ \frac{D-1}{L} & \frac{DR_o}{L} - \frac{(R_{in} + R_o)}{L} \end{bmatrix} \right]^{-1} \quad (15)$$

$$\times \begin{bmatrix} 0 & -\frac{1}{C} \\ \frac{1}{L} & \frac{R_0}{L} \end{bmatrix} \begin{bmatrix} V_o \\ i_L \end{bmatrix}$$

Where:

$$\begin{bmatrix} s & \frac{D-1}{C_o} \\ \frac{1-D}{L} & s - \frac{DR_o}{L} + \frac{(R_{in} + R_o)}{L} \end{bmatrix}^{-1} \quad (16)$$

$$= \frac{1}{s^2 + \left( -\frac{DR_o}{L} + \frac{(R_{in} + R_o)}{L} \right) s + \frac{(D-1)^2}{LC_o}} \times \begin{bmatrix} s - \frac{DR_o}{L} + \frac{(R_{in} + R_o)}{L} & \frac{1-D}{C_o} \\ \frac{D-1}{L} & s \end{bmatrix}$$

If: $s^2 + \left( -\frac{DR_o}{L} + \frac{(R_{in} + R_o)}{L} \right) s + \frac{(D-1)^2}{LC_o} = \Psi \quad (17)$

So:

$$\begin{bmatrix} 0 & 1 \end{bmatrix} \times \begin{bmatrix} \frac{s - \frac{DR_o}{L} + \frac{(R_{in} + R_o)}{L}}{\Psi} & \frac{\frac{1-D}{C_o}}{\Psi} \\ \frac{\frac{D-1}{L}}{\Psi} & \frac{s}{\Psi} \end{bmatrix} = \begin{bmatrix} \frac{\frac{D-1}{L}}{\Psi} & \frac{s}{\Psi} \end{bmatrix} \quad (18)$$

Thus, the resulting transfer function is:

$$\begin{bmatrix} \frac{D-1}{L} & \frac{s}{\Psi} \end{bmatrix} \times \begin{bmatrix} \frac{-i_L}{C_o} \\ \frac{V_o + R_o i_L}{L} \end{bmatrix} = \frac{V_{out}}{D(s)} \quad (19)$$

$$\frac{V_{out}}{D(s)} = -\frac{(D-1)}{\left( s^2 + \left( -\frac{DR_o}{L} + \frac{(R_{in} + R_o)}{L} \right) s + \frac{(D-1)^2}{LC_o} \right) LC_o} i_L + \frac{s}{\left( s^2 + \left( -\frac{DR_o}{L} + \frac{(R_{in} + R_o)}{L} \right) s + \frac{(D-1)^2}{LC_o} \right) LC_o L} V_o \quad (20)$$

So the transfer function that describe behavior of SC port is:

$$G_{SC}(s) = \frac{\hat{V}_{out}}{\hat{D}} = \frac{.5 i_L + s V_o}{8 \times 10^{-7} s^2 + 4 \times 10^{-3} s + .25} \quad (21)$$

**State space average modeling method for battery port**

Fig. 4 shown two operating modes of the battery port. The equations governing the system has been extracted in (22)-(33), then sort out these formulas based on state space variables and the state space is extracted according to (26) and (32). According to the method used in SC half-bridge, the transfer function of the output voltage (Vout) to D, using (11), (12) and

(14) and for battery parameters in accordance table I has been extracted in (33).

$$X=\begin{bmatrix} V_o \\ V_1 \\ i_{Lbatt} \end{bmatrix}, U_i=\begin{bmatrix} I_{out} \\ V_{batt} \end{bmatrix} \quad (22)$$

For Fig. 4.A the equations are:

$$\frac{dV_o}{dt}=\frac{1}{C_o}I_{out} \quad (23)$$

$$V_{batt}=R_{in}i_{Lbatt}+V_1+L_{batt}\frac{di_{Lbatt}}{dt} \Rightarrow \quad (24)$$
$$\frac{di_{Lbatt}}{dt}=\frac{1}{L_{batt}}V_{batt}-\frac{R_{in}}{L_{batt}}i_{Lbatt}-\frac{1}{L_{batt}}V_1$$

$$C_1\frac{dV_1}{dt}+i_{R1}=i_{Lbatt} \;\&\; R_1i_{R1}=V_1 \Rightarrow \quad (25)$$
$$C_1\frac{dV_1}{dt}+\frac{V_1}{R_1}=i_{Lbatt} \Rightarrow \frac{dV_1}{dt}=\frac{1}{C_1}i_{Lbatt}-\frac{1}{R_1C_1}V_1$$

$$\begin{bmatrix} \frac{dV_o}{dt} \\ \frac{dV_1}{dt} \\ \frac{di_{Lbatt}}{dt} \end{bmatrix}=\begin{bmatrix} 0 & 0 & \frac{1}{C_o} \\ 0 & -\frac{1}{R_1C_1} & \frac{1}{C_1} \\ -\frac{1}{L_{batt}} & -\frac{1}{L_{batt}} & -\frac{(R_{in}+R_o)}{L_{batt}} \end{bmatrix}\begin{bmatrix} V_o \\ V_1 \\ i_{Lbatt} \end{bmatrix} \quad (26)$$
$$+\begin{bmatrix} \frac{1}{C_o} & 0 \\ 0 & 0 \\ 0 & \frac{1}{L_{batt}} \end{bmatrix}\begin{bmatrix} I_{out} \\ V_{batt} \end{bmatrix}$$

For Fig. 4.B the equations are:

$$i_{Lbatt}+I_{out}=C_o\frac{dV_o}{dt}, \frac{dV_o}{dt}=\frac{1}{C_o}i_{Lbatt}+\frac{1}{C_o}I_{out} \quad (27)$$

$$i_{R1}+C_1\frac{dV_1}{dt}=i_{Lbatt} \quad \& \quad (28)$$
$$i_{R1}=\frac{V_1}{R1}, \frac{dV_1}{dt}=\frac{1}{C_1}i_{Lbatt}-\frac{1}{R_1C_1}V_1$$

Where:

$$V_{batt}=R_{in}i_{Lbatt}+V_1+L_{batt}\frac{di_{Lbatt}}{dt}+V_{out} \Rightarrow \quad (29)$$
$$\frac{di_{Lbatt}}{dt}=\frac{1}{L_{batt}}V_{batt}-\frac{1}{L_{batt}}V_{out}-\frac{R_{in}}{L_{batt}}i_{Lbatt}-\frac{V_1}{L_{batt}}$$

$$V_{out}=R_oC_o\frac{dV_o}{dt}+V_o=R_oi_{Lbatt}+R_oI_{out}+V_o \quad (30)$$

From (29) and (30):

$$\frac{di_{Lbatt}}{dt}=\frac{1}{L_{batt}}V_{batt}-\frac{(R_{in}+R_o)}{L_{batt}}i_{Lbatt}-\frac{R_o}{L_{batt}}I_{out} \quad (31)$$
$$-\frac{1}{L_{batt}}V_o-\frac{1}{L_{batt}}V_1$$

These matrices are arranged in the following:

$$\begin{bmatrix} \frac{dV_o}{dt} \\ \frac{dV_1}{dt} \\ \frac{di_{Lbatt}}{dt} \end{bmatrix}=\begin{bmatrix} 0 & 0 & \frac{1}{C_o} \\ 0 & -\frac{1}{R_1C_1} & \frac{1}{C_1} \\ -\frac{1}{L_{batt}} & -\frac{1}{L_{batt}} & -\frac{(R_{in}+R_o)}{L_{batt}} \end{bmatrix}\begin{bmatrix} V_o \\ V_1 \\ i_{Lbatt} \end{bmatrix} \quad (32)$$
$$+\begin{bmatrix} \frac{1}{C_o} & 0 \\ 0 & 0 \\ -\frac{R_o}{L_{batt}} & \frac{1}{L_{batt}} \end{bmatrix}\begin{bmatrix} I_{out} \\ V_{batt} \end{bmatrix}$$

From (11), (12) and (14) the transfer function that describe the behavior of battery port is:

$$G_{Batt}(s)=\frac{\hat{V}_{out}}{\hat{D}}=\frac{.06i_{LBatt}+sV_o}{6.1\times10^{-5}s^2+2.25\times10^{-3}s+.33} \quad (33)$$

**Energy Management and Control System**

Proposed EMS has a battery pack and SCs, which are connected through a two input bidirectional DC/DC converter. This converter accomplished by connecting two bidirectional DC-DC converter which can stepping up or stepping down the voltage magnitude. The investigated EMS layout is shown in Fig. 6. In the proposed EMS, a TSSMC passed error signals between the voltages/currents and the references, also the ICA are used for tuning SMC parameters.

Two-surfaces sliding mode controller (TSSMC)

The uncertainty of the proposed EMS is the input voltage and load disturbances and it has two surfaces because of two input sources. It consists of two phases, first, designing an equilibrium surface, such that any state trajectory of the plant restricted to the sliding mode surface is characterized by designed behavior; second, designing a discontinuous control law to force the system to move on the sliding mode surface in a finite time. As soon as the system enters into the sliding mode surface, the controlled system reaches the designed steady state.

Formation of the sliding surface and the control law in terms of circuit parameters make the controller. In order to change the switching frequency of SMC to practical ranges, duty ratio control is adopted. For each port the control law is given by:

$$control\ signal = \mathrm{d} = \mathrm{u} = \begin{cases} 1, s\rangle 0 \\ 0, s\langle 0 \end{cases}, \mathrm{d} = 0.5(1+\mathrm{sgn}(s)) \quad (3)$$

In the proposed EMS the terms of the sliding surface are the battery current error $x_1$ for battery port, the SC current error $x_2$ for SC port, the voltage error $x_3$ and the integrated sum of the two errors $x_4$.

$x_1 = i_{ref}^{Batt} - i_{LBatt}$, $i_{ref}^{Batt} = K_1(v_{ref} - \gamma v_{out})$, $K_1$ is the gain of voltage error

$x_2 = i_{ref}^{SC} - i_L$, $i_{ref}^{SC} = K_2(v_{ref} - \gamma v_{out})$, $K_2$ is the gain of voltage error

$x_3 = v_{ref} - \gamma v_{out}$

$x_4 = \int (x_1, x_2) + x_3$, $x_1$ for battery port and $x_2$ for SC port

Where $K_1$ and $K_2$ are the gain of voltage errors for battery and SC port. Differentiating (39-42) we obtain:

$$\dot{x}_1 = \frac{d\left(i_{ref}^{Batt} - i_{LBatt}\right)}{dt} = \frac{d\left(i_{ref}^{Batt}\right)}{dt} - \frac{d\left(i_{LBatt}\right)}{dt} = -K_1\gamma\frac{I_{c_o}}{c_o} - \frac{d\left(i_{LBatt}\right)}{dt}$$

$$\dot{x}_2 = \frac{d\left(i_{ref}^{SC} - i_L\right)}{dt} = -K_2\gamma\frac{I_{c_o}}{c_o} - \frac{d\left(i_L\right)}{dt}$$

$$\dot{x}_3 = \frac{d\left(v_{ref} - \gamma v_{out}\right)}{dt} = -\gamma\frac{d\left(v_{out}\right)}{dt}$$

$\dot{x}_4 = (x_1, x_2) + x_3$, $x_1$ for battery port and $x_2$ for SC port

By averaging the equations (24) and (31) for battery port in switching period $T_s$:

$$\frac{di_{Lbatt}}{dt} = u\left(\frac{1}{L_{batt}}V_{batt} - \frac{R_{in}}{L_{batt}}i_{Lbatt} - \frac{V_1}{L_{batt}}\right) + (\bar{u})\left(\frac{1}{L_{batt}}V_{batt} - \frac{1}{L_{batt}}V_{out} - \frac{R_{in}}{L_{batt}}i_{Lbatt} - \frac{V_1}{L_{batt}}\right) = \frac{1}{L_{batt}}V_{batt} - \frac{R_{in}}{L_{batt}}i_{Lbatt} - \frac{V_1}{L_{batt}} + \frac{u-1}{L_{batt}}V_{out}$$

So:

$$\dot{x}_1 = -\frac{d\left(i_{LBatt}\right)}{dt} = -\frac{V_{batt}}{L_{batt}} + \frac{R_{in}}{L_{batt}}i_{Lbatt} + \frac{V_1}{L_{batt}} + \frac{(\bar{u})}{L_{batt}}V_{out} - K_1\gamma\frac{I_{c_o}}{c_o}$$

By averaging the equations (2) and (9) for SC port in switching period $T_s$:

$$\frac{di_L}{dt} = u\left(\frac{1}{L}V_{SC} - \frac{R_{in}}{L}i_L\right) + (\bar{u})\left(\frac{1}{L}V_{SC} - \frac{R_{in}}{L}i_L - \frac{V_{out}}{L}\right) = \frac{1}{L}V_{SC} - \frac{R_{in}}{L}i_L - \frac{V_{out}}{L} + \frac{uV_{out}}{L} \quad (45)$$

So:

$$\dot{x}_2 = -\frac{d\left(i_L\right)}{dt} = -\frac{V_{SC}}{L} + \frac{R_{in}}{L}i_L + \frac{(\bar{u})V_{out}}{L} - K_2\gamma\frac{I_{c_o}}{c_o} \quad (46)$$

By irrespective of internal resistance ($R_o$) for capacitor $C_o$:

$$\dot{x}_3 = -\gamma\frac{d\left(v_{out}\right)}{dt} = -\gamma\left(u\left(\frac{-V_{out}}{C_o R_{out}}\right) + (\bar{u})\left(\frac{-V_{out}}{C_o R_{out}} + \frac{(I_L, I_{LBatt})}{C_o}\right)\right) = -\gamma\left(\frac{-V_{out}}{C_o R_{out}} + \frac{(\bar{u})(I_L, I_{LBatt})}{C_o}\right) = \frac{\gamma V_{out}}{C_o R_{out}} - \frac{\gamma(\bar{u})(I_L, I_{LBatt})}{C_o} \quad (47)$$

Where $\bar{u} = 1 - u$ and $u$ has the value 1 if the switch $S_2/S_4$ is on and the value 0 when the switch $S_2/S_4$ is off.

Also:

$$\dot{x}_4 = (x_1, x_2) + x_3 \quad , \quad x_1 \quad (35)$$

for battery port and $x_2$ for SC (36)

port (37)

The instantaneous trajectory of the state variables (38)

for battery port has the expression:

$$S_{Batt} = \alpha_{Batt,1}x_1 + \alpha_{Batt,2}x_3 + \alpha_{Batt,3}x_4 \quad (48)$$

And for SC port:

$$S_{SC} = \alpha_{SC,1}x_2 + \alpha_{SC,2}x_3 + \alpha_{SC,3}x_4 \quad (49)$$

Where $\alpha_{Batt,1}, \alpha_{Batt,2}, \alpha_{Batt3}, \alpha_{SC,1}, \alpha_{SC,2}$ and (40)

$\alpha_{SC,3}$ are the sliding coefficients.

The sliding surface for battery and SC ports are obtained by equaling (49) and (50) with zero: (41)

$$S_{Batt} = \alpha_{Batt,1}x_1 + \alpha_{Batt,2}x_3 + \alpha_{Batt,3}x_4 = 0 \quad (51) \quad (42)$$

$$S_{SC} = \alpha_{SC,1}x_2 + \alpha_{SC,2}x_3 + \alpha_{SC,3}x_4 = 0 \quad (52)$$

## 3. Obtaining Existence Condition

The existence condition ensures that in the vicinity of the sliding surface the state variable trajectories are always directed towards the sliding surface. To guarantee the existence condition, reachability condition given in (53) must be satisfied [37]. (43)

$$\lim_{S\to 0} S\frac{dS}{dt} < 0 \quad (53) \quad (44)$$

This can be expressed as,

$$\frac{dS}{dt}_{S>0} = J^T{}_{(Batt,SC)}Ax + J^T{}_{(Batt,SC)}Bu_{S>0} + J^T{}_{(Batt,SC)}D < 0, \quad u_{S>0} = 1 \quad (54)$$

$$\frac{dS}{dt}_{S<0} = J^T{}_{(Batt,SC)}Ax + J^T{}_{(Batt,SC)}Bu_{S<0} + J^T{}_{(Batt,SC)}D > 0, \quad u_{S<0} = 0 \quad (55)$$

Where $x = \begin{bmatrix} x_1 \\ x_3 \\ x_4 \end{bmatrix}$ for battery port, $x = \begin{bmatrix} x_2 \\ x_3 \\ x_4 \end{bmatrix}$ for SC port, $J^T{}_{Batt} = \begin{bmatrix} \alpha_{Batt,1} & \alpha_{Batt,2} & \alpha_{Batt,3} \end{bmatrix}$ are the sliding coefficients for battery port, $J^T{}_{SC} = \begin{bmatrix} \alpha_{SC,1} & \alpha_{SC,2} & \alpha_{SC,3} \end{bmatrix}$ are the sliding

coefficients for battery port, A, B and D are the state and input matrix.

The existence condition for battery port by replacing (49) in the differentiation of (53) can be obtained as:

$$\frac{dS_{Batt}}{dt}\langle 0 \rightarrow \frac{d(\alpha_{Batt,1}x_1+\alpha_{Batt,2}x_3+\alpha_{Batt,3}x_4)}{dt}\langle 0 \quad for \quad S_{Batt}\rangle 0 \text{ and } \bar{u}=0$$

$$\rightarrow \alpha_{Batt,1}(-\frac{V_{batt}}{L_{batt}}+\frac{R_{in}}{L_{batt}}i_{Lbatt}+\frac{V_1}{L_{batt}}-K_1\gamma\frac{I_{c_o}}{c_o})+\alpha_{Batt,2}(\frac{\gamma V_{out}}{C_oR_{out}})+\alpha_{Batt,3}(x_1+x_3)\langle 0$$

$$\frac{dS_{Batt}}{dt}\rangle 0 \rightarrow \frac{d(\alpha_{Batt,1}x_1+\alpha_{Batt,2}x_3+\alpha_{Batt,3}x_4)}{dt}\rangle 0 \quad for \quad S_{Batt}\langle 0 \text{ and } \bar{u}=1$$

$$\rightarrow \alpha_{Batt,1}(-\frac{V_{batt}}{L_{batt}}+\frac{R_{in}}{L_{batt}}i_{Lbatt}+\frac{V_1}{L_{batt}}+\frac{1}{L_{batt}}V_{out}-K_1\gamma\frac{I_{c_o}}{c_o})+\alpha_{Batt,2}(\frac{\gamma V_{out}}{C_oR_{out}}-\frac{\gamma(\bar{u})I_{LBatt}}{C_o})+\alpha_{Batt,3}(x_1+x_3)\rangle 0$$

The existence condition for SC port by replacing (50) in the differentiation of (53) can be obtained as:

$$\frac{dS_{SC}}{dt}\langle 0 \rightarrow \frac{d(\alpha_{SC,1}x_2+\alpha_{SC,2}x_3+\alpha_{SC,3}x_4)}{dt}\langle 0 \quad for \quad S_{SC}\rangle 0 \text{ and } \bar{u}=0$$

$$\rightarrow \alpha_{SC,1}(-\frac{V_{SC}}{L}+\frac{R_{in}}{L}i_L-K_2\gamma\frac{I_{c_o}}{c_o})+\alpha_{SC,2}(\frac{\gamma V_{out}}{C_oR_{out}})+\alpha_{SC,3}(x_2+x_3)\langle 0$$

$$\frac{dS_{SC}}{dt}\rangle 0 \rightarrow \frac{d(\alpha_{SC,1}x_2+\alpha_{SC,2}x_3+\alpha_{SC,3}x_4)}{dt}\rangle 0 \quad for \quad S_{SC}\langle 0 \text{ and } \bar{u}=1$$

$$\rightarrow \alpha_{SC,1}(-\frac{V_{SC}}{L}+\frac{R_{in}}{L}i_L+\frac{V_{out}}{L}-K_2\gamma\frac{I_{c_o}}{c_o})+\alpha_{SC,2}(\frac{\gamma V_{out}}{C_oR_{out}}-\frac{\gamma(\bar{u})I_L}{C_o})+\alpha_{SC,3}(x_2+x_3)\rangle 0$$

To make the controller as duty ratio controlled circuit, ( $u_{eq}$ ) the equivalent control signal as a function of input $u$ is found from $dS/dt=0$. The equivalent control $u_{eq}$ for each port is obtained by replacing (39-42) in the differentiated equations (51) and (52):

$$\frac{dS_{Batt}}{dt}=0 \rightarrow \frac{d(\alpha_{Batt,1}x_1+\alpha_{Batt,2}x_3+\alpha_{Batt,3}x_4)}{dt}=0$$

$$\rightarrow \alpha_{Batt,1}(-\frac{V_{batt}}{L_{batt}}+\frac{R_{in}}{L_{batt}}i_{Lbatt}+\frac{V_1}{L_{batt}}+\frac{(\bar{u}_{eq}^{Batt})}{L_{batt}}V_{out}-K_1\gamma\frac{I_{c_o}}{c_o}))+\alpha_{Batt,2}(\frac{\gamma V_{out}}{C_oR_{out}}-\frac{\gamma(\bar{u}_{eq}^{Batt})I_{LBatt}}{C_o})+\alpha_{Batt,3}(x_1+x_3)=0$$

$$\frac{dS_{SC}}{dt}=0 \rightarrow \frac{d(\alpha_{SC,1}x_2+\alpha_{SC,2}x_3+\alpha_{SC,3}x_4)}{dt}=0$$

$$\rightarrow \alpha_{SC,1}(-\frac{V_{SC}}{L}+\frac{R_{in}}{L}i_L+\frac{(\bar{u}_{eq}^{SC})V_{out}}{L}-K_2\gamma\frac{I_{c_o}}{c_o})+\alpha_{SC,2}(\frac{\gamma V_{out}}{C_oR_{out}}-\frac{\gamma(\bar{u}_{eq}^{SC})I_L}{C_o})+\alpha_{SC,3}(x_2+x_3)=0$$

Where $\bar{u}_{eq}^{SC}=1-u_{eq}^{SC}$ and $\bar{u}_{eq}^{Batt}=1-u_{eq}^{Batt}$ take values between 0 and 1, so:

$$u_{eq}^{Batt}=1+\frac{\alpha_{Batt,1}(-\frac{V_{batt}}{L_{batt}}+\frac{R_{in}}{L_{batt}}i_{Lbatt}+\frac{V_1}{L_{batt}}-K_1\gamma\frac{I_{c_o}}{c_o})+\alpha_{Batt,2}(\frac{\gamma V_{out}}{C_oR_{out}})+\alpha_{Batt,3}(x_1+x_3)}{(\frac{\alpha_{Batt,1}}{L_{batt}}V_{out}+\alpha_{Batt,2}\frac{-\gamma I_{LBatt}}{C_o})}$$

$$=\frac{V_{out}(\frac{\alpha_{Batt,1}}{L_{batt}}+\frac{\gamma\alpha_{Batt,2}}{C_oR_{out}})+I_{LBatt}(\alpha_{Batt,2}\frac{-\gamma}{C_o}+\alpha_{Batt,1}\frac{R_{in}}{L_{batt}})+(V_1-V_{batt})(\frac{\alpha_{Batt,1}}{L_{batt}})+I_{c_o}(\frac{-\alpha_{Batt,3}K_1\gamma}{c_o})+\alpha_{Batt,3}(x_1+x_3)}{V_{out}(\frac{\alpha_{Batt,1}}{L_{batt}})+I_{LBatt}(\frac{-\gamma\alpha_{Batt,2}}{C_o})}$$

$$u_{eq}^{Batt}(V_{out}(\frac{\alpha_{Batt,1}}{L_{batt}})+I_{LBatt}(\frac{-\gamma\alpha_{Batt,2}}{C_o}))$$

$$=V_{out}(\frac{\alpha_{Batt,1}}{L_{batt}}+\frac{\gamma\alpha_{Batt,2}}{C_oR_{out}})+I_{LBatt}(\alpha_{Batt,2}\frac{-\gamma}{C_o}+\alpha_{Batt,1}\frac{R_{in}}{L_{batt}})+(V_1-V_{batt})(\frac{\alpha_{Batt,1}}{L_{batt}})+I_{c_o}(\frac{-\alpha_{Batt,3}K_1\gamma}{c_o})+\alpha_{Batt,3}(x_1+x_3)$$

If:

$$V_{mts,Batt}=(V_{out}(\frac{\alpha_{Batt,1}}{L_{batt}})+I_{LBatt}(\frac{-\gamma\alpha_{Batt,2}}{C_o})),\ V_{mts,Batt}\times u_{eq}^{Batt}=U_{e,Batt}$$

$$G_{1,\text{Batt}}=\frac{\alpha_{Batt,1}}{L_{batt}}+\frac{\gamma\alpha_{Batt,2}}{C_oR_{out}}$$

$$G_{2,\text{Batt}}=\alpha_{Batt,2}\frac{-\gamma}{C_o}+\alpha_{Batt,1}\frac{R_{in}}{L_{batt}}$$

$$G_{3,\text{Batt}}=\frac{\alpha_{Batt,1}}{L_{batt}}$$

$$G_{4,\text{Batt}}=\frac{-\alpha_{Batt,3}K_1\gamma}{c_o}$$

$$G_{5,\text{Batt}}=\alpha_{Batt,3}$$

Where $V_{mts,Batt}$ is the magnitude of a triangular signal, $G_{1,\text{Batt}}$ , $G_{2,\text{Batt}}$ , $G_{3,\text{Batt}}$ , $G_{4,\text{Batt}}$ and $G_{5,\text{Batt}}$ are the controller coefficients.

Then:

$$U_{e,Batt}=V_{out}(G_{1,\text{Batt}})+I_{LBatt}(G_{2,\text{Batt}})+(V_1-V_{batt})(G_{3,\text{Batt}})+I_{c_o}(G_{4,\text{Batt}})+G_{5,\text{Batt}}(x_1+x_3)$$

And for SC port:

$$u_{eq}^{SC}=1+\frac{\alpha_{SC,1}(-\frac{V_{SC}}{L}+\frac{R_{in}}{L}i_L-K_2\gamma\frac{I_{c_o}}{c_o})+\alpha_{SC,2}(\frac{\gamma V_{out}}{C_oR_{out}})+\alpha_{SC,3}(x_2+x_3)}{(\alpha_{SC,1}\frac{V_{out}}{L}+\alpha_{SC,2}\frac{-\gamma I_L}{C_o})} \quad (56)$$

$$=\frac{V_{out}(\frac{\alpha_{SC,1}}{L}+\frac{\gamma\alpha_{SC,2}}{C_oR_{out}})+I_L(\frac{-\gamma\alpha_{SC,2}}{C_o}+\frac{\alpha_{SC,1}R_{in}}{L})+V_{SC}(\frac{-\alpha_{SC,1}}{L})+I_{c_o}(\frac{-\alpha_{SC,1}K_2\gamma}{c_o})+\alpha_{SC,3}(x_2+x_3)}{V_{out}(\frac{\alpha_{SC,1}}{L})+I_L(\frac{-\gamma\alpha_{SC,2}}{C_o})} \quad (57)$$

$$u_{eq}^{SC}(V_{out}(\frac{\alpha_{SC,1}}{L})+I_L(\frac{-\gamma\alpha_{SC,2}}{C_o}))=$$

$$V_{out}(\frac{\alpha_{SC,1}}{L}+\frac{\gamma\alpha_{SC,2}}{C_oR_{out}})+I_L(\frac{-\gamma\alpha_{SC,2}}{C_o}+\frac{\alpha_{SC,1}R_{in}}{L})+V_{SC}(\frac{-\alpha_{SC,1}}{L})+I_{c_o}(\frac{-\alpha_{SC,1}K_2\gamma}{c_o})+\alpha_{SC,3}(x_2+x_3)$$

If: (58)

$$V_{mts,SC}=(V_{out}(\frac{\alpha_{SC,1}}{L})+I_L(\frac{-\gamma\alpha_{SC,2}}{C_o})),\ V_{mts,SC}\times u_{eq}^{SC}=U_{e,SC} \quad (59)$$

$$G_{1,\text{SC}}=\frac{\alpha_{SC,1}}{L}+\frac{\gamma\alpha_{SC,2}}{C_oR_{out}}$$

$$G_{2,SC}=\frac{-\gamma\alpha_{SC,2}}{C_o}+\frac{\alpha_{SC,1}R_{in}}{L}$$

$$G_{3,\text{SC}}=\frac{-\alpha_{SC,1}}{L}$$

$$G_{4,\text{SC}}=\frac{-\alpha_{SC,1}K_2\gamma}{c_o}$$

$$G_{5,\text{SC}}=\alpha_{SC,3}$$

This can be expressed as:

$$U_{e,SC}=V_{out}(G_{1,\text{SC}})+I_L(G_{2,\text{SC}})+V_{SC}(G_{3,\text{SC}})+I_{c_o}(G_{4,\text{SC}})+G_{5,\text{SC}}(x_2+x_3) \quad (60)$$

Where $V_{mts,\text{SC}}$ is the magnitude of a triangular signal, $G_{1,SC}$ , $G_{2,\text{SC}}$ , $G_{3,\text{SC}}$ , $G_{4,\text{SC}}$ and $G_{5,\text{SC}}$ are the controller coefficients. (61)

Where $x=\begin{bmatrix}x_1\\x_3\\x_4\end{bmatrix}$ for battery port, $x=\begin{bmatrix}x_2\\x_3\\x_4\end{bmatrix}$ for SC port, (62)

$J^T_{Batt}=\begin{bmatrix}\alpha_{Batt,1} & \alpha_{Batt,2} & \alpha_{Batt,3}\end{bmatrix}$ are the sliding coefficients for battery port, (63)

$J^T_{SC}=\begin{bmatrix}\alpha_{SC,1} & \alpha_{SC,2} & \alpha_{SC,3}\end{bmatrix}$ are the sliding coefficients for battery port, A, B and D are the state and input matrix.

The existence condition for battery port by replacing (49) in the differentiation of (53) can be obtained as: (64)

$$\frac{dS_{Batt}}{dt}\langle 0 \rightarrow \frac{d(\alpha_{Batt,1}x_1+\alpha_{Batt,2}x_3+\alpha_{Batt,3}x_4)}{dt}\langle 0 \quad for \quad S_{Batt}\rangle 0 \text{ and } \bar{u}=0$$

$$\rightarrow \alpha_{Batt,1}(-\frac{V_{batt}}{L_{batt}}+\frac{R_{in}}{L_{batt}}i_{Lbatt}+\frac{V_1}{L_{batt}}-K_1\gamma\frac{I_{c_o}}{c_o})+\alpha_{Batt,2}(\frac{\gamma V_{out}}{C_oR_{out}})+\alpha_{Batt,3}(x_1+x_3)\langle 0$$

$$\frac{dS_{Batt}}{dt}\rangle 0 \rightarrow \frac{d(\alpha_{Batt,1}x_1+\alpha_{Batt,2}x_3+\alpha_{Batt,3}x_4)}{dt}\rangle 0 \quad for \quad S_{Batt}\langle 0 \text{ and } \bar{u}=1$$

$$\rightarrow \alpha_{Batt,1}(-\frac{V_{batt}}{L_{batt}}+\frac{R_{in}}{L_{batt}}i_{Lbatt}+\frac{V_1}{L_{batt}}+\frac{1}{L_{batt}}V_{out}-K_1\gamma\frac{I_{c_o}}{c_o})+\alpha_{Batt,2}(\frac{\gamma V_{out}}{C_oR_{out}}-\frac{\gamma(\bar{u})I_{LBatt}}{C_o})+\alpha_{Batt,3}(x_1+x_3)\rangle 0$$

The existence condition for SC port by replacing (50) in the differentiation of (53) can be obtained as:

$$\frac{dS_{SC}}{dt}\langle 0 \rightarrow \frac{d(\alpha_{SC,1}x_2+\alpha_{SC,2}x_3+\alpha_{SC,3}x_4)}{dt}\langle 0 \quad for \quad S_{SC}\rangle 0 \text{ and } \bar{u}=0$$
$$\rightarrow \alpha_{SC,1}(-\frac{V_{SC}}{L}+\frac{R_{in}}{L}i_L-K_2\gamma\frac{I_{c_o}}{c_o})+\alpha_{SC,2}(\frac{\gamma V_{out}}{C_oR_{out}})+\alpha_{SC,3}(x_2+x_3)\langle 0$$
$$\frac{dS_{SC}}{dt}\rangle 0 \rightarrow \frac{d(\alpha_{SC,1}x_2+\alpha_{SC,2}x_3+\alpha_{SC,3}x_4)}{dt}\rangle 0 \quad for \quad S_{SC}\langle 0 \text{ and } \bar{u}=1$$
$$\rightarrow \alpha_{SC,1}(-\frac{V_{SC}}{L}+\frac{R_{in}}{L}i_L+\frac{V_{out}}{L}-K_2\gamma\frac{I_{c_o}}{c_o})+\alpha_{SC,2}(\frac{\gamma V_{out}}{C_oR_{out}}-\frac{\gamma(\bar{u})I_L}{C_o})+\alpha_{SC,3}(x_2+x_3)\rangle 0$$

To make the controller as duty ratio controlled circuit, ( $u_{eq}$ ) the equivalent control signal as a function of input $u$ is found from $dS/dt=0$. The equivalent control $u_{eq}$ for each port is obtained by replacing (39-42) in the differentiated equations (51) and (52):

$$\frac{dS_{Batt}}{dt}=0\rightarrow\frac{d(\alpha_{Batt,1}x_1+\alpha_{Batt,2}x_3+\alpha_{Batt,3}x_4)}{dt}=0$$
$$\rightarrow\alpha_{Batt,1}(-\frac{V_{batt}}{L_{batt}}+\frac{R_{in}}{L_{batt}}i_{Lbatt}+\frac{V_1}{L_{batt}}+\frac{(\bar{u}_{eq}^{Batt})}{L_{batt}}V_{out}-K_1\gamma\frac{I_{c_o}}{c_o}))+\alpha_{Batt,2}(\frac{\gamma V_{out}}{C_oR_{out}}-\frac{\gamma(\bar{u}_{eq}^{Batt})I_{LBatt}}{C_o})+\alpha_{Batt,3}(x_1+x_3)=0$$

$$\frac{dS_{SC}}{dt}=0\rightarrow\frac{d(\alpha_{SC,1}x_2+\alpha_{SC,2}x_3+\alpha_{SC,3}x_4)}{dt}=0$$
$$\rightarrow\alpha_{SC,1}(-\frac{V_{SC}}{L}+\frac{R_{in}}{L}i_L+\frac{(\bar{u}_{eq}^{SC})V_{out}}{L}-K_2\gamma\frac{I_{c_o}}{c_o})+\alpha_{SC,2}(\frac{\gamma V_{out}}{C_oR_{out}}-\frac{\gamma(\bar{u}_{eq}^{SC})I_L}{C_o})+\alpha_{SC,3}(x_2+x_3)=0$$

Where $\bar{u}_{eq}^{SC}=1-u_{eq}^{SC}$ and $\bar{u}_{eq}^{Batt}=1-u_{eq}^{Batt}$ take values between 0 and 1, so:

$$u_{eq}^{Batt}=1+\frac{\alpha_{Batt,1}(-\frac{V_{batt}}{L_{batt}}+\frac{R_{in}}{L_{batt}}i_{Lbatt}+\frac{V_1}{L_{batt}}-K_1\gamma\frac{I_{c_o}}{c_o})+\alpha_{Batt,2}(\frac{\gamma V_{out}}{C_oR_{out}})+\alpha_{Batt,3}(x_1+x_3)}{(\frac{\alpha_{Batt,1}}{L_{batt}}V_{out}+\alpha_{Batt,2}\frac{-\gamma I_{LBatt}}{C_o})}$$
$$=\frac{V_{out}(\frac{\alpha_{Batt,1}}{L_{batt}}+\frac{\gamma\alpha_{Batt,2}}{C_oR_{out}})+I_{LBatt}(\alpha_{Batt,2}\frac{-\gamma}{C_o}+\alpha_{Batt,1}\frac{R_{in}}{L_{batt}})+(V_1-V_{batt})(\frac{\alpha_{Batt,1}}{L_{batt}})+I_{c_o}(\frac{-\alpha_{Batt,1}K_1\gamma}{c_o})+\alpha_{Batt,3}(x_1+x_3)}{V_{out}(\frac{\alpha_{Batt,1}}{L_{batt}})+I_{LBatt}(\frac{-\gamma\alpha_{Batt,2}}{C_o})}$$

$$u_{eq}^{Batt}(V_{out}(\frac{\alpha_{Batt,1}}{L_{batt}})+I_{LBatt}(\frac{-\gamma\alpha_{Batt,2}}{C_o}))$$
$$=V_{out}(\frac{\alpha_{Batt,1}}{L_{batt}}+\frac{\gamma\alpha_{Batt,2}}{C_oR_{out}})+I_{LBatt}(\alpha_{Batt,2}\frac{-\gamma}{C_o}+\alpha_{Batt,1}\frac{R_{in}}{L_{batt}})+(V_1-V_{batt})(\frac{\alpha_{Batt,1}}{L_{batt}})+I_{c_o}(\frac{-\alpha_{Batt,1}K_1\gamma}{c_o})+\alpha_{Batt,3}(x_1+x_3)$$

If:

$$V_{mts,Batt}=(V_{out}(\frac{\alpha_{Batt,1}}{L_{batt}})+I_{LBatt}(\frac{-\gamma\alpha_{Batt,2}}{C_o})),\ V_{mts,Batt}\times u_{eq}^{Batt}=U_{e,Batt}$$
$$G_{1,\mathrm{Batt}}=\frac{\alpha_{Batt,1}}{L_{batt}}+\frac{\gamma\alpha_{Batt,2}}{C_oR_{out}}$$
$$G_{2,\mathrm{Batt}}=\alpha_{Batt,2}\frac{-\gamma}{C_o}+\alpha_{Batt,1}\frac{R_{in}}{L_{batt}}$$
$$G_{3,\mathrm{Batt}}=\frac{\alpha_{Batt,1}}{L_{batt}}$$
$$G_{4,\mathrm{Batt}}=\frac{-\alpha_{Batt,1}K_1\gamma}{c_o}$$
$$G_{5,\mathrm{Batt}}=\alpha_{Batt,3}$$

Where $V_{mts,Batt}$ is the magnitude of a triangular signal, $G_{1,\mathrm{Batt}}$, $G_{2,\mathrm{Batt}}$, $G_{3,\mathrm{Batt}}$, $G_{4,\mathrm{Batt}}$ and $G_{5,\mathrm{Batt}}$ are the controller coefficients. (58)

Then: (59)

$$U_{e,Batt}=V_{out}(G_{1,\mathrm{Batt}})+I_{LBatt}(G_{2,\mathrm{Batt}})+(V_1-V_{batt})(G_{3,\mathrm{Batt}})+I_{c_o}(G_{4,\mathrm{Batt}})+G_{5,\mathrm{Batt}}(x_1+x_3)$$

And for SC port:

$$u_{eq}^{SC}=1+\frac{\alpha_{SC,1}(-\frac{V_{SC}}{L}+\frac{R_{in}}{L}i_L-K_2\gamma\frac{I_{c_o}}{c_o})+\alpha_{SC,2}(\frac{\gamma V_{out}}{C_oR_{out}})+\alpha_{SC,3}(x_2+x_3)}{(\alpha_{SC,1}\frac{V_{out}}{L}+\alpha_{SC,2}\frac{-\gamma I_L}{C_o})}$$
$$=\frac{V_{out}(\frac{\alpha_{SC,1}}{L}+\frac{\gamma\alpha_{SC,2}}{C_oR_{out}})+I_L(\frac{-\gamma\alpha_{SC,2}}{C_o}+\frac{\alpha_{SC,1}R_{in}}{L})+V_{SC}(\frac{-\alpha_{SC,1}}{L})+I_{c_o}(\frac{-\alpha_{SC,1}K_2\gamma}{c_o})+\alpha_{SC,3}(x_2+x_3)}{V_{out}(\frac{\alpha_{SC,1}}{L})+I_L(\frac{-\gamma\alpha_{SC,2}}{C_o})}$$

$$u_{eq}^{SC}(V_{out}(\frac{\alpha_{SC,1}}{L})+I_L(\frac{-\gamma\alpha_{SC,2}}{C_o}))=$$
$$V_{out}(\frac{\alpha_{SC,1}}{L}+\frac{\gamma\alpha_{SC,2}}{C_oR_{out}})+I_L(\frac{-\gamma\alpha_{SC,2}}{C_o}+\frac{\alpha_{SC,1}R_{in}}{L})+V_{SC}(\frac{-\alpha_{SC,1}}{L})+I_{c_o}(\frac{-\alpha_{SC,1}K_2\gamma}{c_o})+\alpha_{SC,3}(x_2+x_3) \quad (60)$$

If:

$$V_{mts,SC}=(V_{out}(\frac{\alpha_{SC,1}}{L})+I_L(\frac{-\gamma\alpha_{SC,2}}{C_o})),\ V_{mts,SC}\times u_{eq}^{SC}=U_{e,SC}$$
$$G_{1,\mathrm{SC}}=\frac{\alpha_{SC,1}}{L}+\frac{\gamma\alpha_{SC,2}}{C_oR_{out}}$$
$$G_{2,SC}=\frac{-\gamma\alpha_{SC,2}}{C_o}+\frac{\alpha_{SC,1}R_{in}}{L} \quad (61)$$
$$G_{3,\mathrm{SC}}=\frac{-\alpha_{SC,1}}{L}$$
$$G_{4,\mathrm{SC}}=\frac{-\alpha_{SC,1}K_2\gamma}{c_o}$$
$$G_{5,\mathrm{SC}}=\alpha_{SC,3}$$

(62)

This can be expressed as:

$$U_{e,SC}=V_{out}(G_{1,\mathrm{SC}})+I_L(G_{2,\mathrm{SC}})+V_{SC}(G_{3,\mathrm{SC}})+I_{c_o}(G_{4,\mathrm{SC}})+G_{5,\mathrm{SC}}(x_2+x_3)$$

Where $V_{mts,\mathrm{SC}}$ is the magnitude of a triangular signal, $G_{1,SC}$, $G_{2,\mathrm{SC}}$, $G_{3,\mathrm{SC}}$, $G_{4,\mathrm{SC}}$ and $G_{5,\mathrm{SC}}$ are the controller coefficients. (63)

## ICA

ICA is a computational method that is used to solve optimization problems of different types. Like most of the methods in the area of evolutionary computation, ICA does not need the gradient of the function in its optimization process. The standard ICA proposed in [45] consists of the following parts: (64)

Generating initial empires (initialization)

Moving the colonies of an empire toward the imperialist (movement of colonies)

Finding the total power of an empire (selection of the new imperialist)

Imperialistic competition (competition between empires to capture colonies)

After a number of iterations only the most powerful empire will remain and this imperialist will control all the countries, which is the optimum solution of the problem (evaluation and elimination of empty empires)

**TSSMC-ICA**

The ICA starts with an initial population which named countries; some of the best countries in the population are selected to the imperialist and the rest form the colonies of these imperialist. All the colonies of initial population are divided among the mentioned imperialists based on their power. Fig. 7 shows the TSSMC-ICA flowchart for tuning TSSMC parameters. In an optimization problem, having an objective function cost (J), the object is to find an argument ‘‘J’’, whose relevant cost is optimum.

$$J = \sum_{i=0}^{n} \left| V_{ref} - \gamma V_{out} \right| \qquad (70)$$

ICA is an evolutionary algorithm which starts with some initial populations, each one called a country [45]. If the optimization problem is N-dimensional, a country is a 1×N array, defined by:

$$country = \left[ p_1, p_2, p_3, p_4, \ldots, p_{Nvar} \right] \qquad (71)$$

Our optimization problem is designing a robust TSSMC controller for controlling the two input bidirectional converter and generating the switching function for each switches, so we generate the initial country that is defined by (72) and the initial matrix of the countries is defined by (73).

$$country_i = \left[ G_{1,i}, G_{2,i}, G_{3,i}, G_{4,i}, G_{5,i} \right], \quad i = SG_{72}Batt \qquad )$$

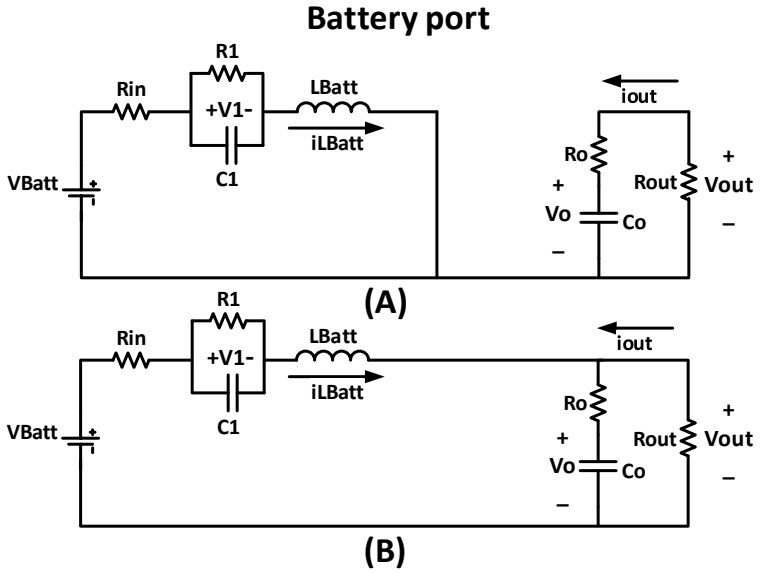


**Fig4.** Two operating modes of the battery port

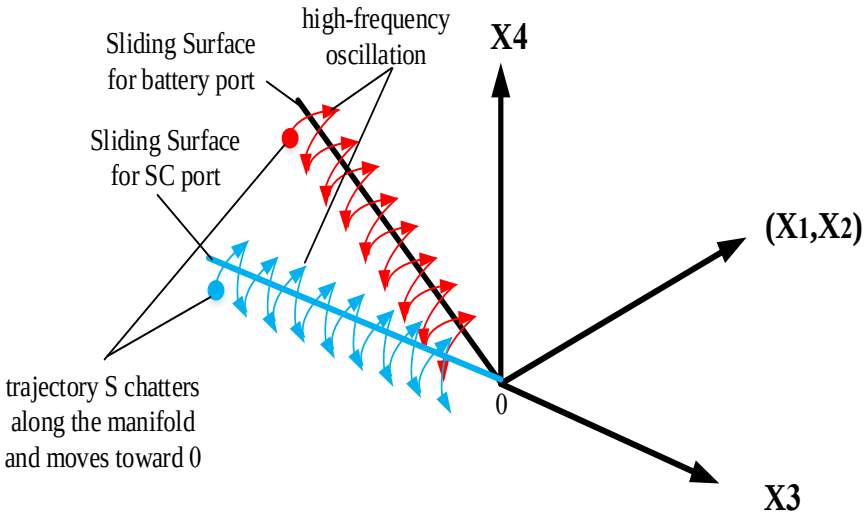


**Fig5.**.Sliding surfaces of TSSMC for each port

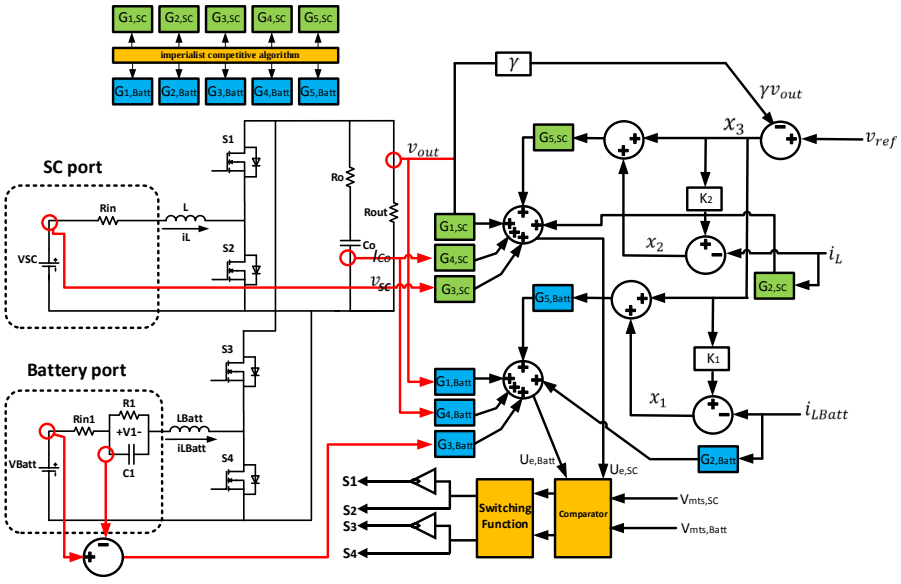


**Fig6.**. The structure of proposed EMS

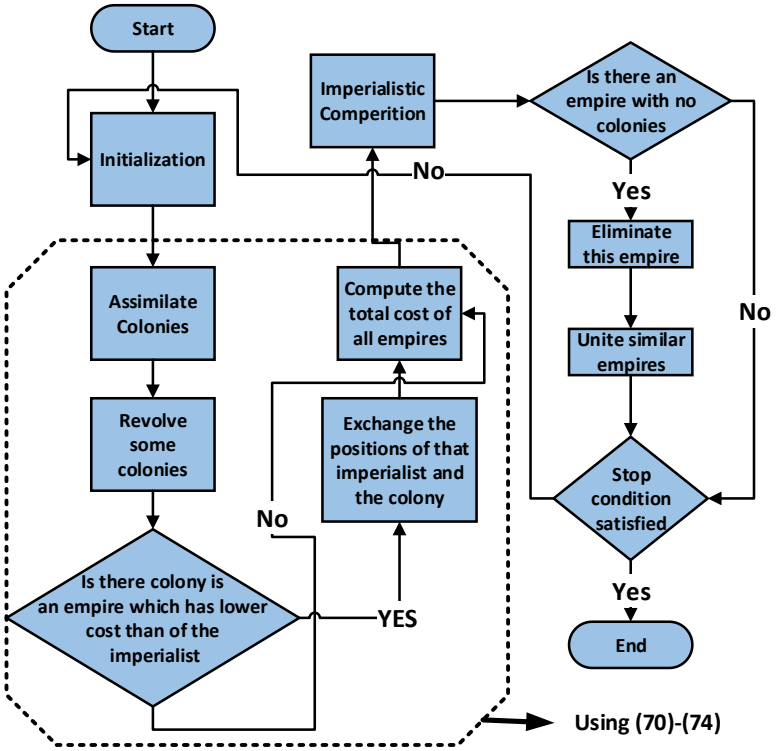


**Fig7.** TSSMC-ICA controller for two input bidirectional converter

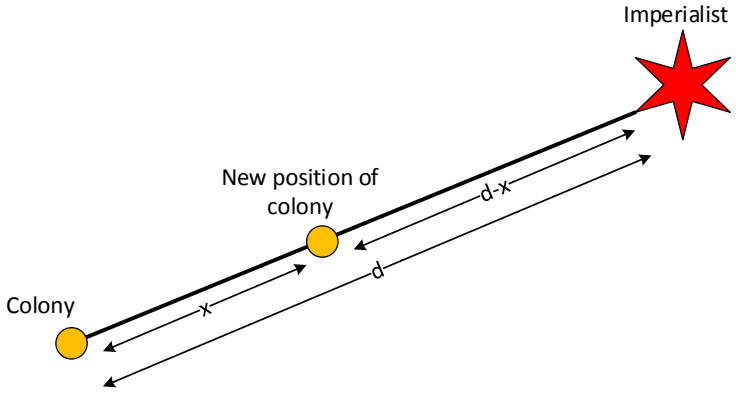


**Fig8.** Moving colonies toward the imperialist

$$country = \begin{bmatrix} country_{Batt,port} \\ country_{SC,port} \end{bmatrix} \quad (73)$$

Imperialist's countries started to improve their colonies. This aim modeled by moving all the colonies toward the imperialist. The new position of colony is shown in Fig. 8. The direction of the movement is the vector from colony to imperialist.

Where:

$$x \sim U\left(0, \beta \times d\right), \beta = number\ greater\ than\ 1,$$
$$d = distance\ between\ colony\ and\ imperialist$$

In order to calculate the cost functions, the initial matrixes of the countries are transferred to the MATLAB environment. There are 600 countries which will result in 600 initial cost functions using 150 iteration. These cost functions are transferred to the ICA algorithm subsequently.

A country with a less cost is deduced as a powerful one, so number of the most powerful ones will be selected to form empires. Rest of them will be the colonies; each of them belongs to an empire. The power of weaker empires will decrease and the power of more powerful ones will increase gradually during imperialistic competition. This competition is modelled by picking some of the weakest empires to initiate a competition among all empires to possess these weak colonies.

The most powerful empires have more chance to possess these colonies. In the competition process, weak empires will lose their colonies and ultimately all the empires except the most powerful one will collapse, so just this unique empire will govern all the colonies in a country which the power and position of its colonies and the empire is identical.

A pseudo-code for TSSMC-ICA is given as bellow:

1) initialization (select some random points of the function and initialize the empires);
2) Due to the (74), moving colonies toward the imperialist;
3) According to the (70), if there is a colony in an empire which has lower cost than that of imperialist, exchange the positions of that colony and the imperialist;
4) Compute the total cost of all empires using (70);
5) Pick the weakest colony from the weakest empire and give it to the empires that has the most likelihood to possess it;
6) Eliminate the powerless empires;
7) If there is just one empire, stop, if not go to first;

System Modeling

In this section, the dynamic models are described for parts of proposed EMS, which consists of lithium-ion battery pack and SC pack. The mathematical models describing the dynamic behavior of each of these components are given below.

Li-ion battery model

Li-Ion batteries are now generally accepted as the best choice for energy [46]. The battery model used in this paper is based on a high-power lithium ion cell [47], which provides high power density and high efficiency. Battery characteristics are determined by internal chemical reactions. These reactions are affected by the ambient temperature (T), the charge-discharge rate and charge-discharge history. The battery characteristics can be modeled as follow:

$$P_{Batt} = P_s + P_{loss}\left(P_s, E_s, T\right) \quad (75)$$

Where Ps is power delivery from battery pack and Ploss is power loss. The battery energy level (Es) is given by (76):

$$E_s\left(t\right) = E_s\left(0\right) + \int_0^t P_s\left(\tau\right) d\tau \quad (76)$$

The current flowing into the battery is determined based on the charging voltage and the internal impedance of the battery [48]. The most common method of SOC calculation that also has been selected in this study is Coulomb-counting. The equations are as follow:

$$SOC = SOC_0 + \frac{1}{C_n}\int_{t_0}^{t} \left|i_{Batt}\right| dt, During\ \ Charging \quad (77)$$

$$SOC = SOC_0 - \frac{1}{C_n}\int_{0}^{t} \left|i_{Batt}\right| dt, During\ \ Discharging \quad (78)$$

This method needs an accurate measurement of battery current (iBatt) and knowing the initial value of SOC (SOC0).

The dynamic model of battery is presented in Fig. 9, where VtBatt is the cell terminal voltage and Rin is a lumped resistance due to cell interconnections. A double layer capacitance C1 is shown in parallel with the charge transfer polarization represented by R1. It should be noted that the battery open circuit voltage (VBatt) and lumped resistance (Rin) are strongly dependent on battery SOC.

## 4. SC model

The power density of the SC is considerably higher than the battery; this is due to the fact that the charges are physically stored on the electrodes. Low internal resistance gives SC high efficiency but can result in a large burst of output currents if the SC is charged at a very low SOC [49]. Another feature of the SC is that the terminal voltage is directly proportional to the SOC. As shown in Fig. 10, the SCs are modeled as a series connection of a SC open circuit voltage (VSC) and an initial resistor (Rin). The output current of SC can be modeled as follow:

$$i_{SC} = \frac{V_{SC} \pm \sqrt{{V_{SC}}^2 - 4P_r R_{int}}}{2R_{int}},\ P_r\ is\ power\ request \quad (79)$$

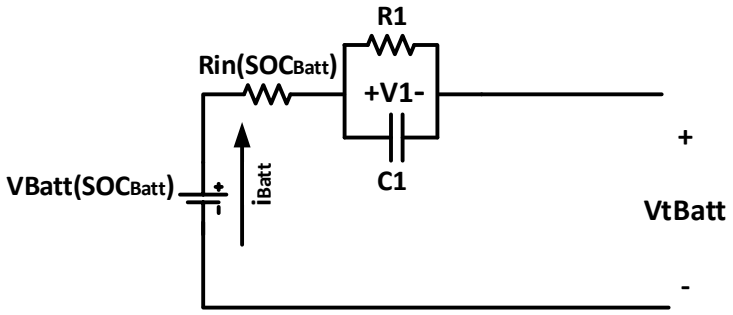


**Fig9.** Simplified equivalent circuit of the battery

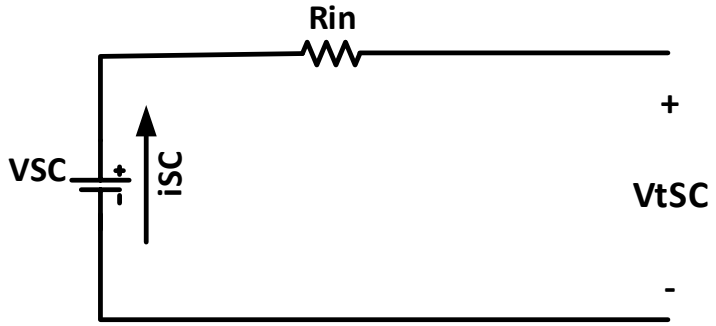


**Fig10.** Equivalent circuit of a SC

## 5. Simulation Results and Discussion

In order to verify the effects of proposed EMS, all the components were modeled in MATLAB/SIMULINK environment, then, the performance of EV which equipped with proposed EMS was investigated through simulation in two cases: a) in case of fixed input voltages (with and without disturbances) ; b) in case of the stochastic EV driving cycle. As illustrated in (80), energy required by the electric motor is always balanced by the proposed original control algorithm.

$$P_{load} = P_{SC} + P_{Batt} \quad (80)$$

### Fixed input voltages (with and without disturbances)

The proposed EMS works in two operations, discharging mode and charging mode (regenerative braking). In EVs, regenerative braking is a system that utilizes the mechanical energy from the motor by converting kinetic energy into electrical energy and fed back to the sources of energy. In an EV, when regenerative braking occurs, the speed is reduced and the electric machine can operate as a generator.

For these two modes, the proposed TSSMC-ICA controller passed error signals between the voltages/currents and the references. For discharging mode the converters step-up stages are used to step up the storage voltages; the current in the battery/SC arises from the transfer of electrons from one electrode to the other.

During discharging, the oxidation reaction at the anode generates electrons and reduction reaction at the cathode uses these electrons; therefore during discharging, electrons flow from the anode to the cathode. In discharging mode, when the switch S2/S4 is on, the battery/SC supplies energy to the battery/SC inductor (L).

When the switch S2/S4 is off, the output capacitor CO receives energy from the inductor as well as from the battery/SC. Thereby, the voltage at the output capacitor terminals can be regulated accordingly with the motor speed by adjusting the duty-cycle of the switch S2/S4. Whenever either the reference value for the motoring current is set to zero or the EV braking command is issued, the switch S2/S4 is turned off and kept in this state till the braking command is removed and a reference value greater than zero is commanded for the motoring current. Hence, when the switch

S2/S4 is permanently off the battery/SC output current goes to zero because of the instantaneous difference between the voltage Vout and battery/SC voltage which reverse biases the diode. After a fixed blanking time interval the switch S1/S3 is turned on to allow the reversal of the power flow. Thereafter, the switch S1/S3 is operated at constant switching frequency and variable duty-cycle in order to keep at the desired value the braking current flowing in the storage elements.

For charging mode (regenerative braking), the vehicle energy is accomplished by using the converter step down stages, which give a path for the braking current and allow the recovery of the vehicle energy in the storages, it must be noted that in this mode when the switch S1/S3 is on, the battery/SC receives energy from the capacitor CO as well as from the motor, which operates as a generator at expenses of the vehicle kinetic energy. By turning off the switch S1/S3 the storage elements are isolated from such an energy supply, and thereby the control of the average value of the braking current flowing in the battery can be accomplished by regulating the duty cycle of the switch S1/S3.

For any of these two operations, the switches S1 and S2 or S3 and S4 are never operated at the same time, being the switch S1/S3 always off during motoring operation, in order to avoid a shoot through, whereas the switch S2/S4 is kept off continuously whenever the regenerative braking operation is commanded. Figs. 11 and 12, respectively show the output voltage of the SC port and the output voltage of the battery port when using the proposed TSSMC-ICA controller, in case of fixed input voltages (with low and high disturbances and without disturbances). Fig. 13 shows the output voltage response of the proposed TSSMC method under load disturbance from 15 to 8 Ohm. Fig. 14 shows Ueq,SC, Ueq,Batt, PWM for switch S2 and PWM for switch S4.

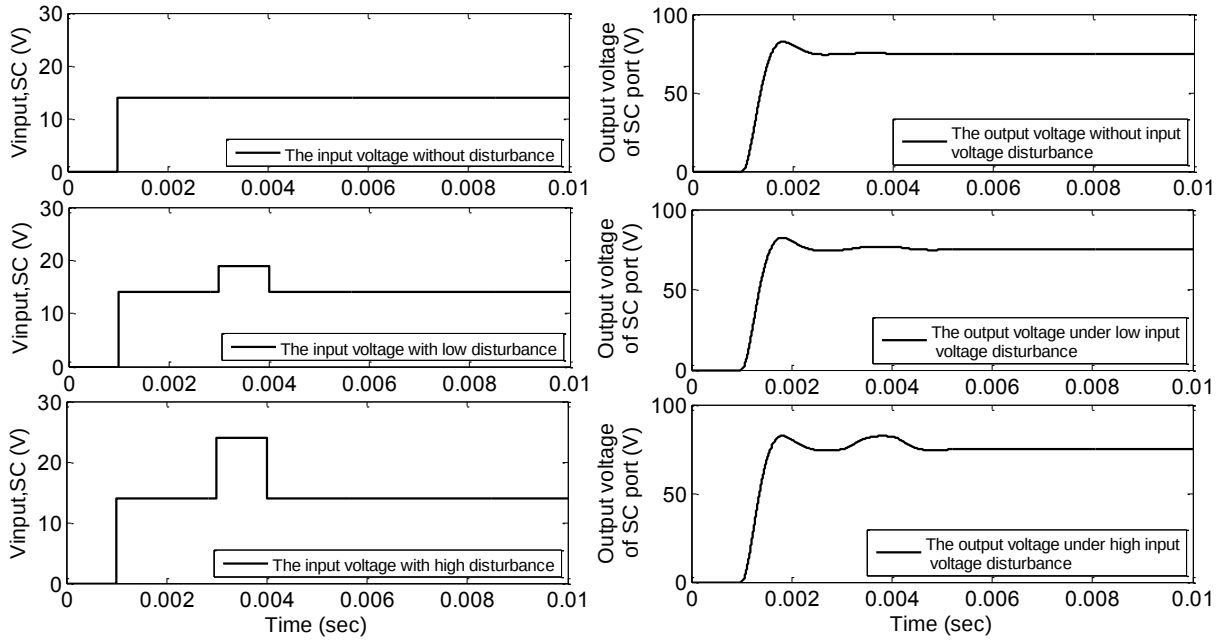


**Fig11.** The output voltage of the SC port under different input voltage disturbances

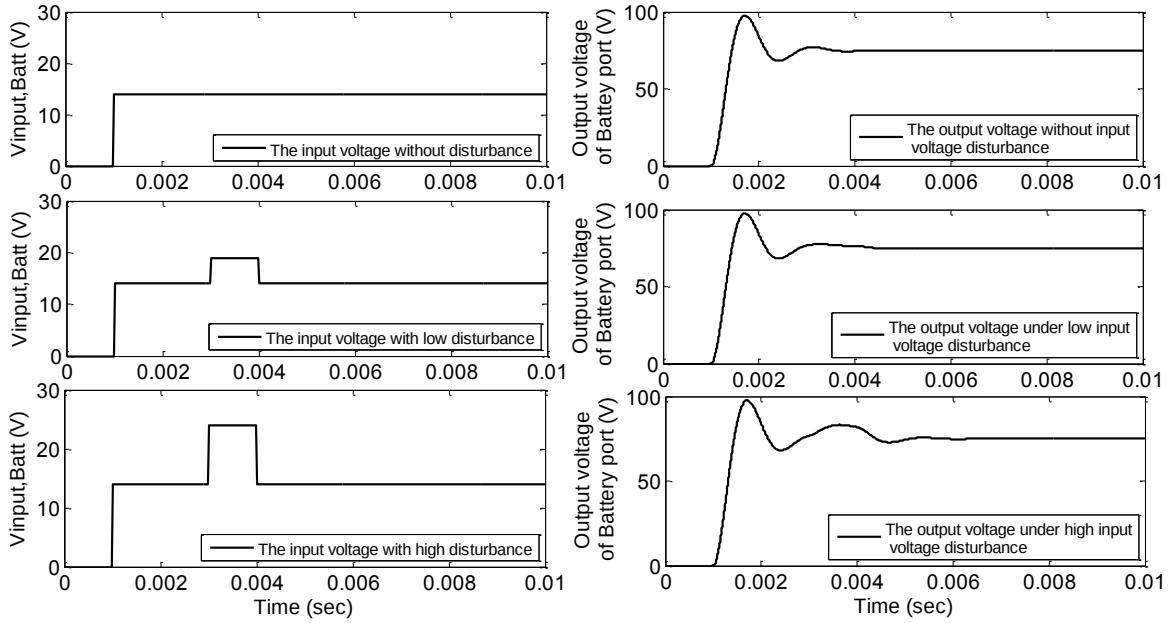


**Fig12.** . The output voltage of the battery port under different input voltage disturbances

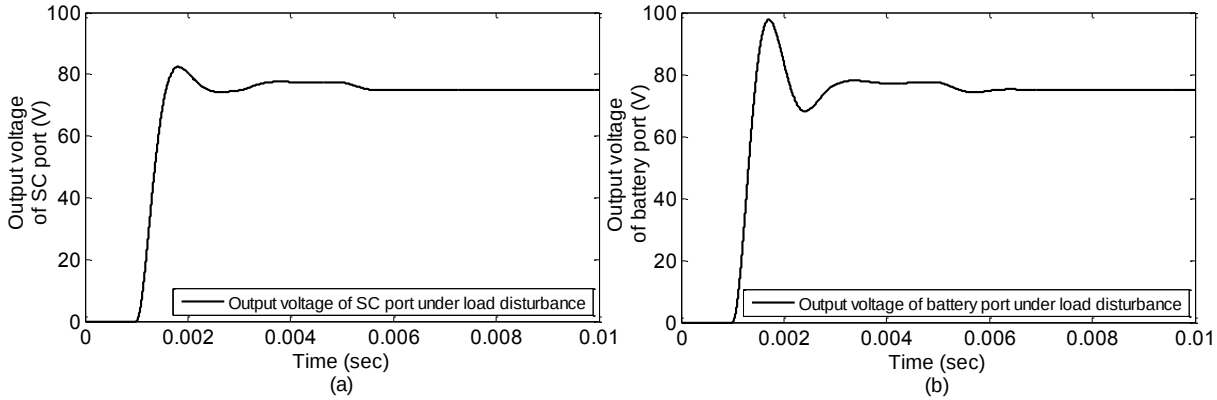


**Fig13.** The output voltage response of the proposed TSSMC method under load disturbance, a) SC port; b) battery port

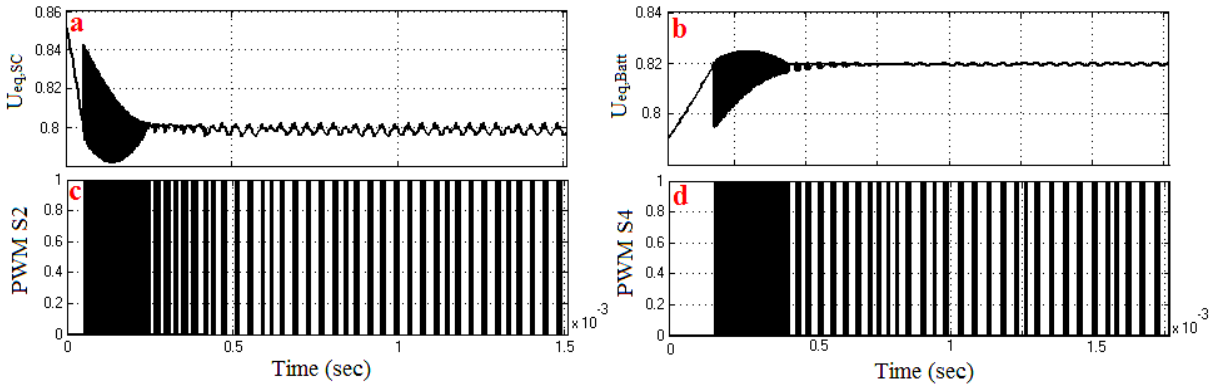


**Fig14.** . a) Ueq,SC; b) Ueq,Batt; c) PWM for switch S2 (SC port); d) PWM for switch S4 (battery port)

**Stochastic EV driving cycle**

As illustrated in Fig. 15, in this section the performance of EV which equipped with proposed EMS was investigated through simulation in case of the stochastic EV driving cycle. Battery health management plays a vital role in defining the state of health of battery based on different aging processes. Rapid loss of power and sudden rise of temperature are some examples of events that reduce the battery life.

Fig. 16 shows the output battery current along with SC pack with proposed EMS and the output battery current without SC pack. When the SCs is not installed in the system the peak current is 196A and the working current of the battery varied greatly, which will reduce the operating life of the battery and tend to generate extensive heat inside the battery, which leads to increased battery internal resistance, thus lower efficiency and ultimately premature failure.

When the SC is coupled with the battery with proposed EMS, it is clear from Fig. 16 that the battery peak current is decreased to 100 A. In addition, there are fewer spikes of current from the battery, therefore producing a steadier current. Without the SC's assistance, there are ten spikes of current above 50 A, with the addition of the SC, there is only three spike of current above 50 A, with one other close.

When the current from the battery is closer to a constant value with fewer spikes, the battery has a potential for an increased efficiency and life expectancy, further reducing the cost of the energy source and actual power loss in the EMS.

Therefore, as can be seen from Fig. 17 the value of SOC with and without SC at the same amount of battery charge are different.

The DC-link voltage of proposed EMS is shown in Fig. 18. According to this figure, by combining the TSSMC and ICA, the energy storage device is delivered a smooth line voltage to the motor, furthermore the voltage spikes are so little. As shown in Fig. 19 in order to verify the improvement of energy indices, at the end of 1000 second efficiency of proposed EMS with TSSMC-ICA and pure SMC was compared.

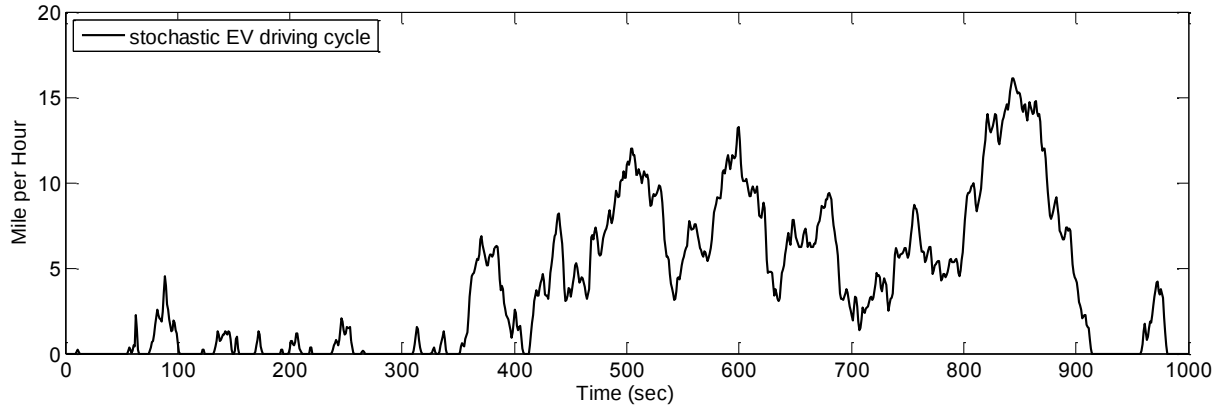


**Fig15.** Stochastic EV driving cycle

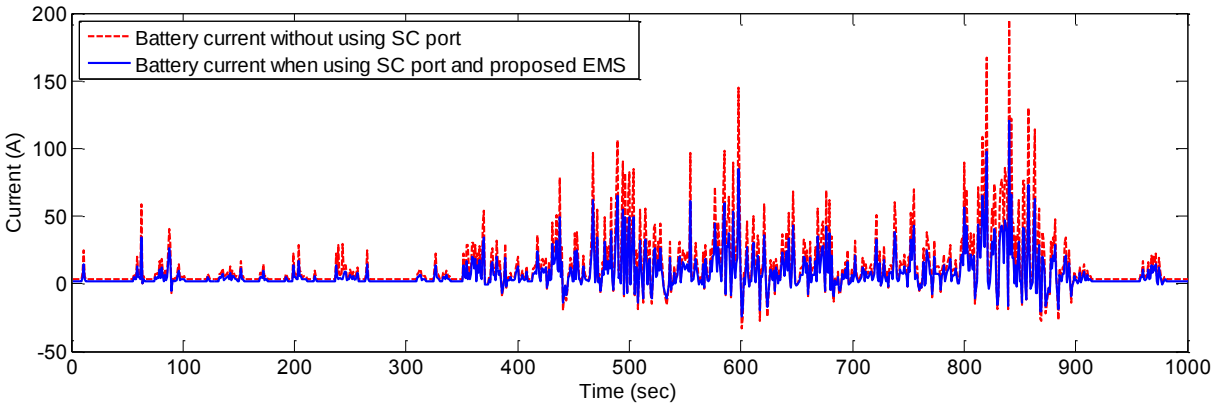


**Fig16.** Comparison of battery pack current (along with SC pack using proposed EMS and without using SC pack)

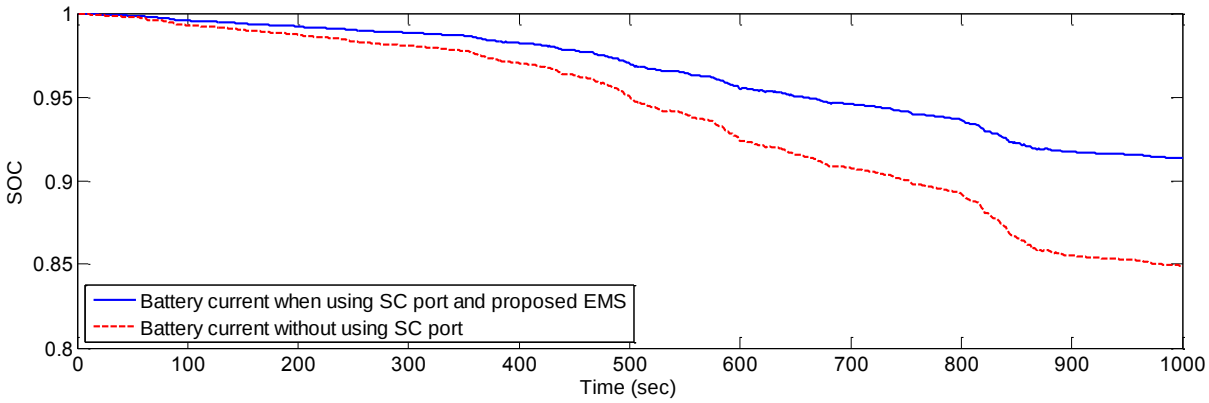


**Fig17.** Comparison of battery pack SOC (along with SC pack using proposed EMS and without using SC pack)

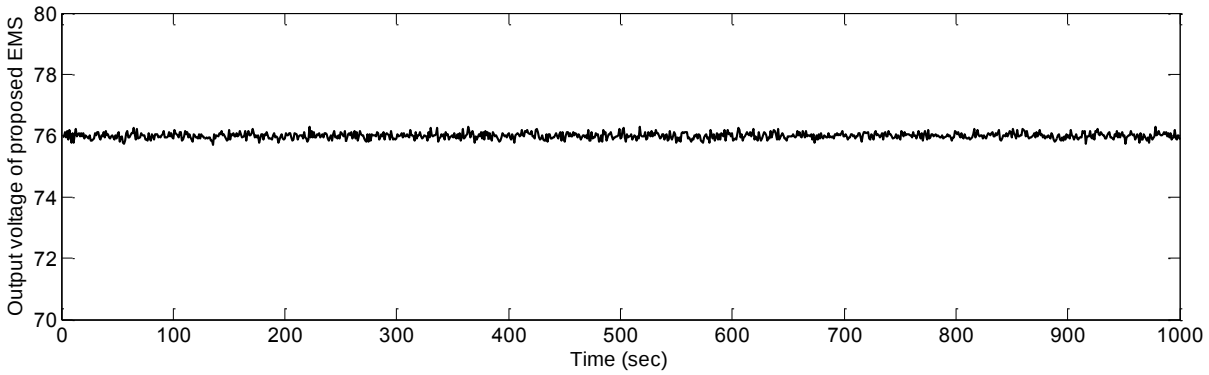


**Fig18.** Output voltage of proposed EMS

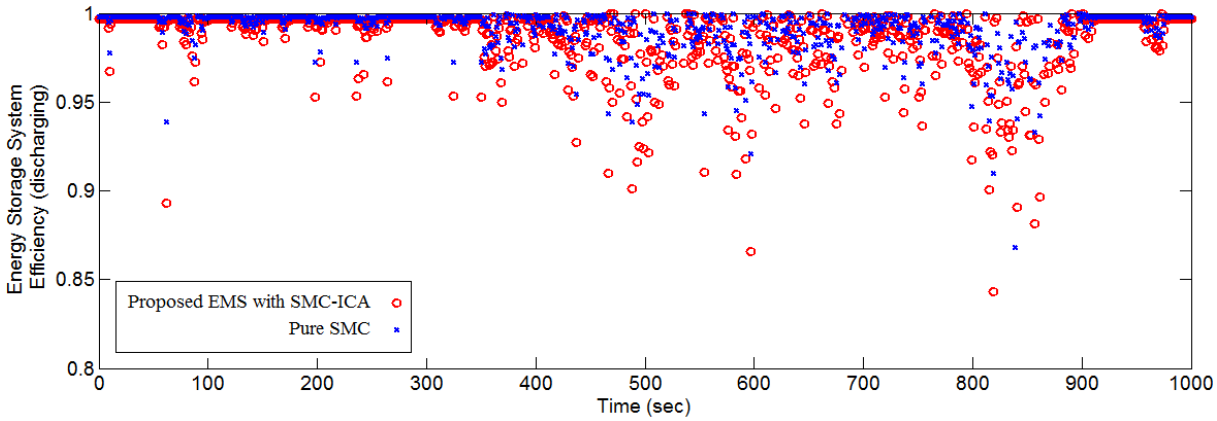


**Fig19.** . Comparison efficiency of proposed EMS with TSSMC-ICA and pure SMC

## Conclusion

In this work, a new two input sources EMS with novel controller which combining the TSSMC and ICA based feedback control of an ESS to be used in EV applications has been proposed. Each storage port are controlled directly through a sliding mode controller based on ICA. The purpose of the EMS consists of Li-Ion battery, SC bank and two input bidirectional DC-DC converter. For modeling the equations governing the system, state-space average modeling technique was used. The results show that the proposed method can effectively improve the performance of EV power control and follow a desired output power for electric motor. The proposed EMS has continuous input and output current; hence reduced ripple current in the output.

**References**


[1]. A. Emadi, "Advanced Electric Drive Vehicles ", CRC Press, Oct., 2014.

[2]. Z. Qian, O. Abdel-Rahman and I. Batarseh, "An integrated four-port DC/DC converter for renewable energy applications," IEEE Trans. vol. 25, no. 7, pp. 1877-1887, Jul. 2010.

[3]. N. Zhang, D. Sutanto and K. M. Muttaqi, "A review of topologies of three-port DC–DC converters for the integration of renewable energy and energy storage system", Renewable and Sustainable Energy Reviews, vol. 56, pp. 388–401, April 2016.

[4]. H. Wu, K. Sun, S. Ding and Y. Xing, "Topology derivation of non-isolated three-port DC–DC converters from DIC and DOC", IEEE Trans Power Electron, vol. 28, no. 7, pp. 3297–3307, 2013.

[5]. S. Ding, H. Wu, Y. Xing, Y. Fang and X. Ma, "Topology and control of a family of non-isolated three-port DC/DC converters with a bidirectional cell", Proceedings of APEC, pp.1089–1094, 2013.

[6]. L. Wang, Z. Wang and H. Li, "Asymmetrical duty cycle control and decoupled power flow design of a three-port bidirectional DC-DC converter for fuel cell vehicle application", IEEE Trans Power Electron; vol. 27, no. 2, pp. 891-904, 2012.

[7]. J. Xie, X. Zhang, C. Zhang and S. Liu, "A novel three-port bidirectional DC/DC converter", Proceedings of PEDG, pp. 717-720, 2010.

[8]. H. Al-Atrash, F. Tian, and I. Batarseh, "Tri-modal half-bridge converter topology for three-port interface," IEEE Trans. Power Electron., vol. 22, no. 1, pp. 341-345, Jan. 2007.

[9]. Z. Qian, O. Abdel-Rahman, and I. Batarseh, "An Integrated four-port DC/DC converter for renewable energy application," IEEE Trans. Power Electron., vol. 25, no. 7, pp. 1877-1887, Jul. 2010.

[10]. G. Wen, Y. Chen and Y. Kang, "A family of cost-efficient integrated single-switch three-port converters", Proceedings of APEC, pp. 1062–1067, 2013.

[11]. H. Zhu, D. Zhang, B. Zhang and Z. Zhou," A non-isolated three-port DC–DC converter and three-domain control method for PV-battery power systems", IEEE Transaction on Industrial Electronics, vol. 62, no. 8, pp. 4937–4947, 2015.

[12]. N. Vazquez, C. Sanchez, C. Hernandez, E. Vazquez and R. Lesso, "A three-port converter for renewable energy applications", Proceedings of ISIE, pp. 1735-1740, 2011.

[13]. Y. Chen, G. Wen, L. Peng, Y. Kang and J. Chen, "A family of cost-efficient non-isolated single-inductor three-port converters for low power stand-alone renewable power applications", Proceedings of APEC, pp. 1083–1088, 2013.

[14]. Y. Chen, P. Zhang, X. Zou, Y. Kang, "Dynamical modelling of the non-isolated single-inductor three-port converter", Proceedings of APEC, pp. 2067-2073, 2014.

[15]. Son, Y.I., Kim, I.H.: 'Complementary PID controller to passivity-based nonlinear control of boost converters with inductor resistance', IEEE Trans. Control Syst. Technol., vol. 20, no. 3, pp. 826–834, 2012.

[16]. Guo, L., Hung, J.Y., Nelms, R.M.: 'Comparative evaluation of sliding mode fuzzy controller and PID controller for a boost converter', Electr. Power Syst. Res., vol. 81, no. 1, pp. 99–106, 2011.

[17]. Chan, C.Y.: 'Development of non-linear controllers for a tri-state boost converter', IET Power Electron., vol. 5, no. 1, pp. 68–73, 2012.

[18]. Alvarez-Ramirez, J., Cervantes, I., Espinosa-Perez, G.: 'A stable design of PI control for DC-DC converters with an RHS zero', IEEE Trans. Circuits Syst., 2001, vol. 48, no. 1, pp. 103–106, 2001.

[19]. Kapat, S., Krein, P.T.: 'Formulation of PID control for DC–DC converters based on capacitor current: a geometric context', IEEE Trans. Power Electron., vol. 27, no. 3, pp. 1424–1432, 2012.

[20]. Chan, C.Y.: 'Comparative study of current-mode controllers for a high-order boost dc–dc converter', IET Power Electron., 2013, 7, (1), pp. 237–243

[21]. 21Leyva, R., Alonso, C., Queinnec, I., Tarbouriech, S.: 'Passivity-based integral control of a boost converter for large-signal stability', IEE Proc. Control Theory Appl., vol. 153, no. 2, pp. 139–146, 2005.

[22]. Wai, R., Shih, L.: 'Design of voltage tracking control for DC–DC boost converter via total sliding-mode technique', IEEE Trans. Ind. Electron., 2011, vol. 58, no. 6, pp. 2502–2511, 2011.

[23]. Alexandridis, A.T., Konstantopoulos, G.C.: 'Non-linear voltage regulator design for DC/DC boost converters used in photovoltaic applications: analysis and experimental results', IET Renew. Power Gener., vol. 7, no. 3, pp. 296–308, 2013

[24]. Wai, R., Shih, L.: 'Adaptive fuzzy-neural-network design for voltage tracking control of a DC–DC boost converter', IEEE Trans. Power Electron.,vol. 27, no. 4, pp. 2104–2115, 2012.
[25]. Beid, S.E.l., Doubabi, S.: 'DSP-based implementation of fuzzy output tracking control for a boost converter', IEEE Trans. Ind. Electron., vol. 61, no. 1, pp. 196–209, 2014.
[26]. Sundareswaran, K., Sreedevi, V.T.: 'Boost converter controller design using queen-bee-assisted GA', IEEE Trans. Ind. Electron., 2009, 56, (3), pp. 778–783
[27]. Nelms, R.M.: 'Fuzzy logic average current-mode control for DC-DC converters using an inexpensive 8-bit microcontroller'. IEEE Industry Applications Conf., Seattle, USA, pp. 2615–2622, 2004.
[28]. Wang, Y-X., Yu, D-H., Kim, Y-B.: 'Robust time-delay control for the DC–DC boost converter', IEEE Trans. Ind. Electron., 2014, 61, (9), pp. 4829–4837
[29]. Chan, C.Y.: 'Analysis and experimental study of an output feedback controller for a high-order boost dc–dc converter', IET Power Electron., vol. 6, no. 7, pp. 1279–1287, 2013.
[30]. Shirazi, M., Zane, R.: 'An autotuning digital controller for DC – DC power converters based on online frequency-response measurement', IEEE Trans. Power Electron., vol. 24, no. 11, pp. 2578–2588, 2009.
[31]. Morroni, J., Corradini, L., Zane, R.: 'Adaptive tuning of switched-mode power supplies operating in discontinuous and continuous conduction modes', IEEE Trans. Power Electron., vol. 24, no. 11, pp. 2603–2611, 2009.
[32]. Corradini, L., Mattavelli, P., Stefanutti, W.: 'Simplified model reference-based autotuning for digitally controlled SMPS', IEEE Trans. Power Electron., vol. 23, no. 4, pp. 1956–1963, 2008.
[33]. Olalla, C., Leyva, R., El Aroudi, A., Queinnec, I.: 'Robust LQR control for PWM converters: an LMI approach', IEEE Trans. Ind. Electron., vol. 56, no. 7, pp. 2548–2558, 2009.
[34]. Olalla, C., Leyva, R., El Aroudi, A., Garcés, P, Queinnec, I.: 'LMI robust control design for boost PWM converters', IET Power Electron., vol. 3, no. 1, pp. 75–85, 2010.
[35]. Montagner, V.F., Maccari, L.A., Oliveira, R.C.L.F., Pinheiro, H.: 'Robust H2 control applied to boost converters: design, experimental validation and performance analysis', IET Control Theory Appl., vol. 6, no. 12, pp. 1881–1888, 2012.
[36]. Vidal-Idiarte, E., Martinez-Salamero, L., Calvente, J.: 'An H∞ control strategy for switching converters in sliding-mode current control', IEEE Trans. Power Electron., vol. 21, no. 2, pp. 553–556, 2006.
[37]. A. Babya and M. Nithya, "Sliding Mode Controlled Forward Converter", IEEE Sponsored 9th International Conference on Intelligent Systems and Control (ISCO), pp. 1-4 ,2015.
[38]. S. K. Kollimalla, M. Mishra and N. Narasamma, "Design and Analysis of Novel Control Strategy for Battery and Supercapacitor Storage System" IEEE Transaction on sustainable energy, vol. 5, no. 4, 2014.
[39]. P. Thounthong, S. Pierfederici, J.P. Martin, M. Hinaje, and B. Davat, "Modeling and Control of Fuel Cell/Supercapacitor Hybrid Source Based on Differential Flatness Control" IEEE Transaction on vehicular technology, vol. 59, no. 6, 2010.
[40]. L. Fangcheng, L. Jinjun, Z. Bin, Z. Haodong and H. S. Ul, "Energy Management of Hybrid Energy Storage System (HESS) Based on Sliding Mode Control" IEEE on 7th International Power Electronics and Motion Control Conference, Harbin, China, 2012.
[41]. R. A. DeCarlo, S. H. Zak, and G. P. Matthews, "Variable structure control of nonlinear multivariable systems: A tutorial," Proc. IEEE, vol. 76, pp. 212–234, 1988.
[42]. V. I. Utkin, Sliding Mode and Their Application in Variable Structure Systems. Moscow, U.S.S.R.: MIR, 1978.
[43]. H. S. Ramirez, "Differential geometric methods in variable-structure control," Int. J. Control, vol. 48, no. 4, pp. 1359–1390, 1988.
[44]. R. D. Middlebrook, "A general unified approach to modeling switching-converter power stages," Proc. IEEE Power Electronics Specialists Conf., pp. 18-34, 1976.
[45]. E. A. Gargari and C. Lucas, "Imperialist competitive algorithm: an algorithm for optimization inspired by imperialist competition", IEEE Congress on Evolutionary Computation, pp. 4661-4667, 2007.
[46]. A. Burke, "Batteries and ultracapacitors for electric, hybrid, and fuel cell vehicles," Proceedings of the IEEE, vol. 95, no. 4, pp. 806-820, 2007.
[47]. A123 Systems. [Online]. Available: http://www.a123systems.com.
[48]. D. A. J. Rand, R. Woods and R. M. Dell, "Batteries for Electric Vehicles", Research Studies Press Ltd, pp. 125– 230, 1998.